ICTAC Kinetics Committee recommendations for analysis of multi-step kinetic

Sergey Vyazovkin, Alan K. Burnham, Loïc Favergeon, Nobuyoshi Koga, Elena Moukhina, Luis A.Pérez-Maqueda, Nicolas Sbirrazzuoli

ICTAC Kinetics Committee recommendations for analysis of multi-step kinetics

Sergey Vyazovkin[*1], Alan K. Burnham[2], Loic Favergeon[3], Nobuyoshi Koga[4], Elena Moukhina[5], Luis A. Pérez-Maqueda[6], Nicolas Sbirrazzuoli[7]

[1]Department of Chemistry, University of Alabama at Birmingham, 901 S. 14th Street, Birmingham, AL 35294, USA
[2]Alan Burnham Consultant, 4221 Findlay Way, Livermore, CA 94550, USA
[3]Mines Saint-Etienne, University of Lyon, CNRS, UMR 5307 LGF, Centre SPIN, F-42023 Saint-Etienne, France
[4]Department of Science Education, Graduate School of Education, Hiroshima University, 1-1-1 Kagamiyama, Higashi-Hiroshima 739-8524, Japan
[5]NETZSCH-Gerätebau GmbH, Wittelsbacherstrasse 42, Selb, 95100, Germany
[6]Instituto de Ciencia de Materiales de Sevilla, C.S.I.C–Universidad de Sevilla, C. Américo Vespucio No. 49, 41092 Sevilla, Spain
[7]University Côte d'Azur, Institute of Chemistry of Nice, UMR CNRS 7272, 06100 Nice, France

Abstract.
The present recommendations have been developed by the Kinetics Committee of the International Confederation for Thermal Analysis and Calorimetry (ICTAC). The recommendations provide guidance on kinetic analysis of multi-step processes as measured by thermal analysis methods such as thermogravimetry (TGA) and differential scanning calorimetry (DSC). Ways of detecting the multi-step kinetics are discussed first. Then, four different approaches to evaluation of kinetic parameters (the activation energy, the pre-exponential factor, and the reaction model) for individual steps are considered. The approaches considered include multi-step model-fitting as well as distributed reactivity, isoconversional, and deconvolution analyses. For each approach practical advice is offered on its effective usage. Due attention is also paid to the typical problems encountered and to the ways of resolving them. The objective of these recommendations is to help a non-expert with efficiently performing multi-step kinetic analysis and interpreting its results.

Keywords: crystallization, decomposition, degradation, polymerization, pyrolysis

CONTENTS

Foreword

This publication continues the series of the ICTAC Kinetics Committee recommendations for improving the quality of kinetic analysis. The first two publications have dealt respectively with selecting proper computational techniques [1] and obtaining adequate experimental data [2]. The present publication provides recommendations devoted specifically to kinetic analysis of multi-step processes. The idea of creating such recommendations was discussed at length in a kinetics session at the 16th Congress of ICTAC (Orlando, USA, 2016). During this session several approaches to multi-step kinetic analysis were identified. They include multi-step model-fitting, distributed reactivity, isoconversional, and deconvolution analyses. The development of the present recommendations was led by the chair of the Kinetics Committee, Sergey Vyazovkin, who is listed as the first author. Other team members are listed in the alphabetical order. The specific contributions were as follows: Multi-step model-fitting (Moukhina); Distributed reactivity analysis (Burnham); Isoconversional analysis (Vyazovkin and Sbirrazzuoli); Deconvolution analysis (Koga, Perez-Maqueda, and Favergeon). The approaches described are considered to be generally independent. Thus, the order of appearance of the respective sections does not follow any specific plan.

The draft document was sent to a number of expert reviewers with a request to provide comments. The comments were received from thirteen individuals mentioned in Acknowledgements of this document. In response to the reviewers' comments, revisions were made to clarify the existing content rather than to expand it, so that the document remained focused on its major objective. The latter was to provide a newcomer to the field of thermal analysis kinetics with introductory pragmatic guidance in efficiently applying common computational approaches to kinetic analysis of multi-step processes.

1. Introduction

The methods of thermal analysis such as thermogravimetric analysis (TGA) and differential scanning calorimetry (DSC) are used broadly to study the kinetics of processes in the condensed (i.e., liquid or solid) phases. The condensed phase processes typically include more than a single step. For example, under the action of heat an organic solid can convert to gaseous products via competition of decomposition and sublimation, i.e., intra- and inter molecular bond breaking, respectively. On the other hand, thermal polymerization can occur as a sequence of two steps: diffusion of the monomer followed by its addition to the polymer

chain. These are just two simple examples of multi-step processes that can give rise to multi-step kinetics. Yet, the typical approach to kinetic analysis of the condensed phase processes is based on the single-step rate equation [1]:

$$\frac{d\alpha}{dt} = k(T)f(\alpha) = A\exp\left(\frac{-E}{RT}\right)f(\alpha) \tag{1.1}$$

where α is the extent of conversion of the reactant to products, t is the time, T is the absolute temperature, $k(T)$ is the Arrhenius rate constant, A is the preexponential factor, E is the activation energy, R is the gas constant, and $f(\alpha)$ is the reaction model. A list of common reaction models is found elsewhere [1]. A combination of A, E, and $f(\alpha)$ is frequently called the kinetic triplet. Note that there is a tendency to limit kinetic analysis to estimating the activation energy only. Undoubtedly, in many situations a change in the activation energy can explain a change in the reaction rate. Nevertheless, there are just as many situations when the rate changes can only be explained by changes in the preexponential factor and/or reaction model [3,4,5]. Therefore, kinetic analysis should generally aim at determining the whole kinetic triplet.

The fact that a condensed phase process is likely to include more than one step does not immediately invalidate the application of the single-step approach. Quite commonly multi-step kinetics can be accurately approximated as the single-step ones. It happens when the overall rate of the multi-step process is either dominated or limited by the rate of one step. Consider the two aforementioned examples. The overall rate is determined by the sum of the rates of sublimation and decomposition but the former can be much faster than the latter. Then the overall rate is dominated by the fastest step, i.e., sublimation. On the other hand, in polymerization occurring as two consecutive steps the rate of diffusion can be much slower than the rate of the monomer addition. Then the overall rate of polymerization is limited by a single step of diffusion.

How can one recognize multi-step kinetics in TGA and/or DSC data? The simplest and most obvious way is by visual inspection of the curves. For a single step process the TGA curve obtained at constant rate of heating should be S-shaped (sigmoidal) with a single inflection point. Similarly, the DSC curve obtained at constant rate of heating or cooling should be a single bellshaped peak with no shoulders. The same is true for the derivate of TGA data commonly referred to as DTG, i.e., derivative thermogravimetry. Therefore, if a TGA curve shows more than one inflection point, i.e., looks like an overlap of two or more S-shaped curves, the process is certainly not single-step. For DTG and DSC curves the appearance of more than one peak or a peak with one or more shoulders clearly signals that the process is not single step. As an illustration, Figure 1 shows TGA and DSC curves for the thermal decomposition of acetylsalicylic acid [6]. The TGA curve is clearly an overlap of two S-shaped segments. The DSC curve demonstrates three endothermic peaks, the first of which is melting followed by a double peak for thermal decomposition. The results of this type suggest that the process comprises at least two steps. Thus, a two-step kinetic model should be used as a starting point in analysis of the overall kinetics of such process. It should be noted that the aforementioned features of multi-step kinetics are not always obvious, and that the chances of detecting them increase with extending the range of experimental conditions. In particular, one has better chances to detect these features when using a broader temperature range. This is easier to accomplish via nonisothermal measurements, for which one is recommended to use close to ten-fold difference between the slowest and fastest heating (or cooling) rates [2].

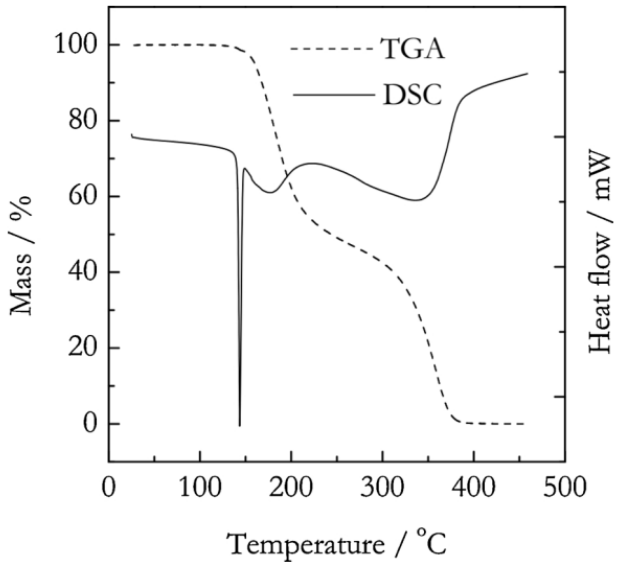

Fig. 1. TGA (dash line) and DSC (solid line) curves for thermal decomposition of acetylsalicylic acid. Adapted with permission from Long et al. [6]. Copyright 2002 Wiley.

Unfortunately, the visual inspection does not always reveal the multi-step nature of a process even within a broad temperature range. There are many situations when multi-step processes do not exhibit any of the features described above, i.e., give rise to the single-step type of the DSC and TGA curves. Therefore, the absence of double peaks, peak shoulders, and overlapped S-shaped segments should not be taken as proof of the underlying kinetics being single step. A more effective way of recognizing multi-step kinetics is via simple single-step kinetic analysis. The idea behind this approach is quite straightforward. The activation energy of a process is determined from the temperature dependence of its rate. In particular, it can be determined as the isoconversional derivative of the overall rate, i.e., as [1]:

$$E_\alpha = -R\left[\frac{\partial \ln(d\alpha/dt)}{\partial T^{-1}}\right]_\alpha \tag{1.2}$$

where the subscript α denotes the values related to a given conversion. The application of such derivative to a single-step equation (1.1) yields $E_\alpha = E$. It means that the experimentally determined value of the isoconversional activation energy, E_α remains constant regardless of the values of conversion and temperature. In theory, the constancy of E_α is the necessary condition for treating a process as single-step kinetics. In practice, E_α is never exactly constant. Thus the criterion of constancy is replaced by the criterion of insignificant variation. Variation in E_α can be considered insignificant when it is smaller than the respective uncertainty. Typical uncertainties in evaluating $E\alpha$ are ± 5-10% of E_α. Then variation in E_α is insignificant if the difference between the maximum and minimum value of E_α is less than 10 – 20 % of the average E_α value. When applying this criterion, one should keep in mind that the E_α values typically are subject to larger fluctuations at $\alpha < 0.1$ and $\alpha > 0.9$. Therefore, the constancy (or significant variability) are best judged by analyzing the values within the range α=0.1-0.9. It should be emphasized that the constancy of $E\alpha$ does not necessarily mean that the reaction is a single-step one. More likely, it is a multi-step reaction whose rate is dominated or limited by one of the steps, as explained earlier.

Normally, the constancy of E_α does not hold when a process involves more than one step. Let us consider a process that comprises two competing steps:

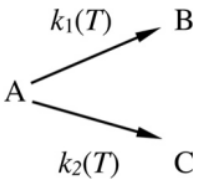

(1.3)

The overall rate of this process is:

$$\frac{d\alpha}{dt} = k_1(T)f_1(\alpha) + k_2(T)f_2(\alpha) \tag{1.4}$$

where the subscript 1 and 2 represents respectively the two individual steps. Applying the isoconversional derivative to this rate gives the isoconversional activation energy as follows:

$$E_\alpha = \frac{E_1 k_1(T)f_1(\alpha) + E_2 k_2(T)f_2(\alpha)}{k_1(T)f_1(\alpha) + k_2(T)f_2(\alpha)} \tag{1.5}$$

Eq. 1.5 obviously suggests that the resulting activation energy depends on temperature as well as on conversion. Depending on the values of α and T, E_α can take on any value between E_1 and E_2, i.e., between the values of the activation energies of the two steps. Therefore, as long as E_1 and E_2 differ significantly, and the rates of the steps are comparable (i.e., there is no rate dominating step), the multi-step nature of the process is likely to manifest itself as either conversion or temperature dependence of the experimentally determined activation energy. The conversion dependence of the experimental activation energy is readily determined by an isoconversional method. There is a number of isoconversional methods, and their basic overview is given in the previous ICTAC recommendations [1]. Figure 2 illustrates an application of one such method to the process of crosslinking polymerization in an epoxy-anhydride system [7]. Note that visual inspection of the DSC curves does not reveal any obvious features of a multi-step process. Nevertheless, the isoconversional activation energy varies significantly indicating clearly that the kinetics of this process cannot be described as a single step.

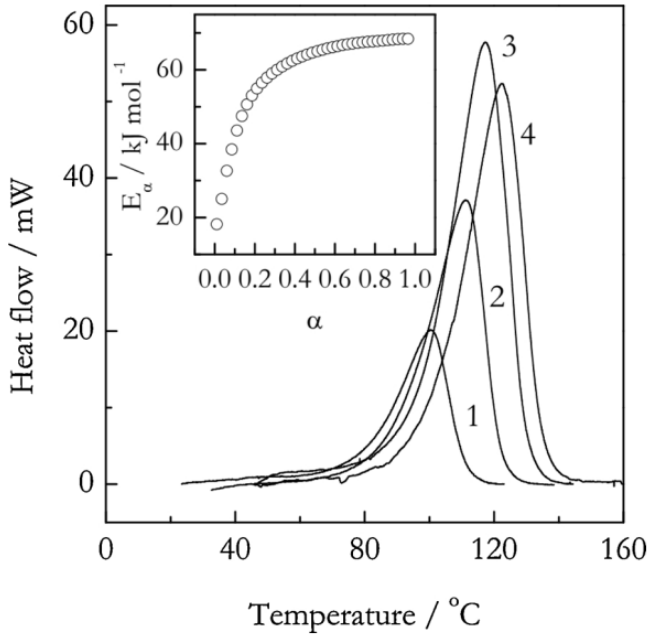

Fig. 2. DSC curves for crosslinking polymerization of an epoxy-anhydride system. The numbers by the curves are heating rates in °C min^{-1}. The inset shows the conversion dependence of the isoconversional activation energy. Adapted with permission from Vyazovkin and Sbirrazzuoli [7]. Copyright 1999 Wiley-VCH.

The temperature dependence of the experimental activation energy can be detected from the Arrhenius plot, i.e., $\ln k(T)$ vs T^{-1}. When the activation energy varies with temperature, the plot is nonlinear. Arrhenius plots are used more commonly in analysis of isothermal data. For nonisothermal data, a close analog of the Arrhenius plot is the Kissinger plot. The latter is the basis of the Kissinger method [8,9] that affords evaluating the activation energy as:

$$E = -R\frac{d\ln\left(\frac{\beta}{T_p^2}\right)}{dT_p^{-1}} \tag{1.6}$$

where β is the heating rate, and the subscript p denotes the temperature related to the position of the maximum (or minimum) of a DSC or DTG peak. Figure 3 displays the Kissinger plot for the thermal denaturation of collagen [10]. The plot is distinctly nonlinear. The activation energy determined for the lower temperature range is markedly greater than the one found at higher temperatures. This is a clear indication that the kinetics of the process cannot be reduced to a single step. Again, visual inspection of the DSC curves for this process does not reveal any signs of it being multi-step [10]. It should be stressed that detecting the nonlinearity of the Kissinger plots requires using no less than five different heating rates [10,11,12]. Similar requirement applies to the Arrhenius plots for isothermal data. It is very difficult to detect the nonlinearity when using fewer than five different temperatures. When using the Kissinger method, one should consider comparing the plot of $\ln(\beta/T_p^2)$ vs. T_p^{-1} with the plot that replaces β/T_p^2 with the width of the normalized rate peak at the half-height. If the slops of these plots yield significantly different values of the activation energy, this is a sign of a multi-step process [13].

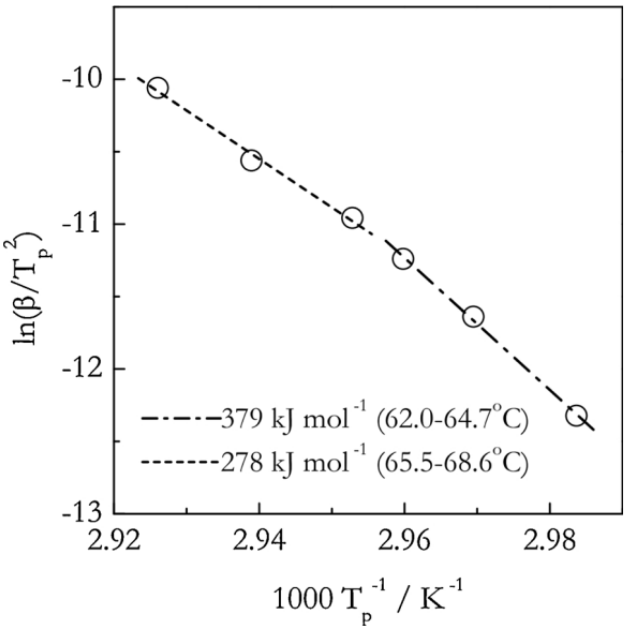

Fig. 3. Kissinger plot for the thermal denaturation of collagen. Dash-dot and dash lines represent two approximately linear segments that correspond to lower (62.0–64.7°C) and higher (65.5–68.6°C) temperature regions of the overall nonlinear plot. The respective values of the activation energy are 379 and 278 kJ mol^{-1}. Adapted with permission from Vyazovkin et al. [10]. Copyright 2007 Wiley-VCH.

As a summary, it must be stressed that one should never rely exclusively on visual inspection of the DSC or TGA curves to judge whether a process constitutes multi-step kinetics. As explained above, multi-step kinetics can give rise to the single-step type of the DSC and TGA curves. In this circumstance, one is advised to examine the data by a method capable of

revealing the multi-step nature of a process. The use of an isoconversional method is preferred over that of Kissinger because it is more sensitive in detecting kinetic complexity and equally applicable to isothermal and nonisothermal data. It is essential that any method used employs multiple heating rates or, more generally, multiple temperature programs. This has been the major recommendation of the ICTAC Kinetics Committee [1]. It does remain in force for analysis of multi-step kinetics. All the approaches discussed further are based on this recommendation. Similarly, one should follow the recommendations [2] on collecting high quality kinetic data. The more complex a process under study the higher data quality is needed for its successful kinetic analysis.

Last but not least, multi-step kinetics studies can always benefit from obtaining mechanistic information. Microscopic examination can reveal distinct heterogeneity in a solid reactant or product that can hint at the occurrence of parallel reaction channels. XRD analysis of the solid phase at different stages of the reaction progress can detect intermediate products that indicates the presence of consecutive steps. Similar information can be furnished by FTIR or Raman spectroscopy of the liquid phase. MS and FTIR analysis of the gas phase products and a change in their distribution during the reaction can provide important insights into the identity of the reaction steps involved into the overall process. The mechanistic information is of great help in both developing and interpreting multi-step kinetic models.

However, one should be aware of the fundamental difference between a multi-step reaction mechanism and a kinetic model that describes it. The mechanisms of even relatively simple reactions may involve a dozen or more steps. This does not mean that a kinetic model must include all these steps. Furthermore, an attempt to build a model that includes that many steps to describe a set of TGA and/or DSC data is nearly guaranteed to fail in estimating reliable kinetic parameters of the individual steps. Instead, one should strive building a model that includes the fewest number of steps, yet can describe the kinetics accurately in a wide range of experimental conditions. Most of the time, multi-step reaction mechanisms can be accurately described by a reaction model that includes two or three steps. It is an important task of a kinetic study to understand which steps of a multi-step reaction mechanism determine the reaction kinetics under specific experimental conditions.

2. Multi-step model-fitting

2.1 Basics

For each chemical reaction, the kinetic analysis means evaluation of the kinetic triplet, i.e., E, A and $f(\alpha)$. Although there is a single kinetic triplet for a single-step reaction (see eq. 1.1), for a multi-step reaction the number of kinetic triplets equals the number of the steps. For multi-step reactions, kinetic analysis has an additional task of establishing the multi-step kinetic model. The latter specifies a connection between the reaction steps and is determined by the reaction mechanism. The steps can be independent or can interact with each other. The steps can interact in a variety of manners. They can be competing (eq. 1.3) or consecutive, i.e., when a reactant forms an intermediate before transforming into the final product. Individual steps can appear separately or simultaneously. In either case, the overall reaction rate, i.e., the rate of conversion of the initial reactants to final products is the sum of the reaction rates of the individual reaction steps. In multi-step kinetic analysis, it is assumed that each reaction step i has its own extent of conversion α_i, reaction rate $d\alpha_i/dt$, activation energy E_i, pre-exponential factor Ai, and reaction model $f_i(\alpha_i)$ [14]. Each step includes a reactant and a product. The step is an independent one if its reactant and product are not involved in other steps of the multi-step kinetic model. Steps are consecutive if a product of one step is a reactant of another step. Steps are competing if they involve the same reactant [15]. A multi-step reaction can contain the steps that are connected in different ways. For example, decomposition of 2,2'-azobisisobutyronitrile (AIBN) [16,17] involves three steps, the step $A \rightarrow B$ represents

decomposition in the solid phase, and a competitive channel $A \rightarrow C \rightarrow D$ that exhibits melting ($A \rightarrow C$) followed by decomposition in the liquid phase ($C \rightarrow D$). In addition to its own conversion and rate, each step is represented by its specific contribution (or weight) w_i to the overall conversion and rate. For the same multi-step reaction, the values of the weights can be different for different types of measurements (e.g., DSC vs TGA). For example, endothermic and exothermic steps in a multi-step decomposition [18] have positive w_i contributions to the mass loss (TGA), whereas their contributions to the heat flow signal (DSC) have the opposite signs. Similarly, in Figure 1 the melting step at 150°C would have a significant contribution to the total heat flow, but zero contribution to the total mass loss. In general, the overall conversion and rate are determined as:

$$\alpha = \sum_i w_i \alpha_i \tag{2.1}$$

$$\frac{d\alpha}{dt} = \sum_i w_i \frac{d\alpha_i}{dt} \tag{2.2}$$

These equations are independent of the connections between individual steps in the multi-step kinetic model. The total conversion (Eq. 2.1) is determined experimentally as the ratio of either partial mass loss (TGA) or a partial heat release (DSC) to the total mass loss (TGA) or to the total heat release (DSC). If a step $R_i \rightarrow P_i$ refers to an individual reaction step for conversion of the reactant R_i to the product P_i, its reaction rate depends on the current relative amounts of the respective species C_{Ri} and C_{Pi}, in accord with the following equation:

$$\frac{d\alpha_i}{dt} = k_i(T) f_i(C_{Ri}, C_{Pi}) \tag{2.3}$$

Here, the relative amounts C_R and C_P of the reactant R and the product P are dimensionless values between 0 and 1. They are defined as the ratio of the current amount of reactant to the maximum theoretically possible amount of this reactant during the progress of the whole reaction. For a single-step reaction, C_P has the same meaning as α, and C_R is (1-α). In the absence of autocatalysis (i.e., when the product does not react with the reactant) the reaction rate of each step depends only on the relative amount of this step reactant. Then the relative amount in eq. 2.3 can be replaced with conversions that vary from 0 to 1. For a single-step reaction, the sum of C_P and C_R is always 1. In the case of multi-step reactions, the relative amounts of the reactant and product reactants of a selected step can be influenced by other steps so that the sum C_P+C_R could be less than 1. However, in any given sequence of consecutive steps, the sum of all relative amounts of all reactants in the sequence is equal to 1. At the beginning of a multi-step reaction, the relative amount of the starting reactant in each consecutive chain is equal to 1, and the relative amount of all intermediate and final products are equal to zero. In a multi-step reaction, the relative amount of a starting reactant is decreased by all steps that involve this reactant. Thus, in the case of two competing steps (eq. 1.3), the rate of decrease for the relative amount of the reactant A is determined as:

$$\frac{dC_A}{dt} = -k_1(T) f_1(C_A, C_B) - k_2(T) f_2(C_A, C_C) \tag{2.4}$$

For n competing steps the rate becomes:

$$\frac{dC_A}{dt} = -\sum_i^n k_i(T) f_i(C_A, C_{Pi}) \tag{2.5}$$

The relative amount of each product is then increased as follows

$$\frac{dC_{Pi}}{dt} = k_i(T) f_i(C_A, C_{Pi}) \tag{2.6}$$

When a multi-step reaction involves the formation of intermediate, its relative amount is increased by the steps in which this intermediate is a product, and decreased by the steps in which it is a reactant. For example, for the following multi-step kinetic model:

$$A \xrightarrow{k_1} B \underset{k_3}{\overset{k_2}{\rightarrow}} \begin{matrix} C \\ D \end{matrix} \tag{2.7}$$

The relative amount of the intermediate product B is calculated as:

$$\frac{dC_B}{dt} = k_1(T) f_1(C_A, C_B) - k_2(T) f_2(C_B, C_C) - k_3(T) f_3(C_B, C_D) \tag{2.8}$$

In general, the equation for the relative amount change in each reactant contains *n* steps for its increase and m steps for its decrease:

$$\frac{dC_i}{dt} = +\sum_{j}^{n} k_j(T) f_j(C_j, C_i) - \sum_{l}^{m} k_l(T) f_l(C_i, C_l) \tag{2.9}$$

The complete system of equations for a multi-step reaction consists of:

- Kinetic Equations (2.3) for all individual steps.
- Rate of relative amount change for each reactant in the multi-step kinetic model, Equation (2.9).
- Balance Equation (2.1) for calculation of the overall conversion or overall conversion rate Equation (2.2) for all steps.

In order to solve this system, one has to assume the number of steps, the multi-step kinetic model with connections of the steps, and the reaction model $f(\alpha)$ for each step. Mathematical solution of this system of differential equations calculates the simulated curve $\alpha(t)$, which can be compared with the experimental curve. The unknown parameters in this system are optimized to accomplish the best fit to the experiment that produces the following results:

- r^2 (the coefficient of determination) and RSS (the residual sum of squares) to characterize the goodness of fit
- w_i, E_i, and A_i for each step
- other unknown parameters of the reaction model for each step such as reaction order (n_i), order of autocatalysis (m_i), Avrami exponent (p_i),

Advantage of the model-fitting method is that it is readily applicable for analysis of strongly overlapping steps, independent or competing steps, overlapped exothermic and endothermic peaks, reactions where changing of the reaction mechanism happens at different conversion values (see Figure 4), crosslinking polymerization with diffusion control due to vitrification as well as in the situations when the total effect cannot be measured.

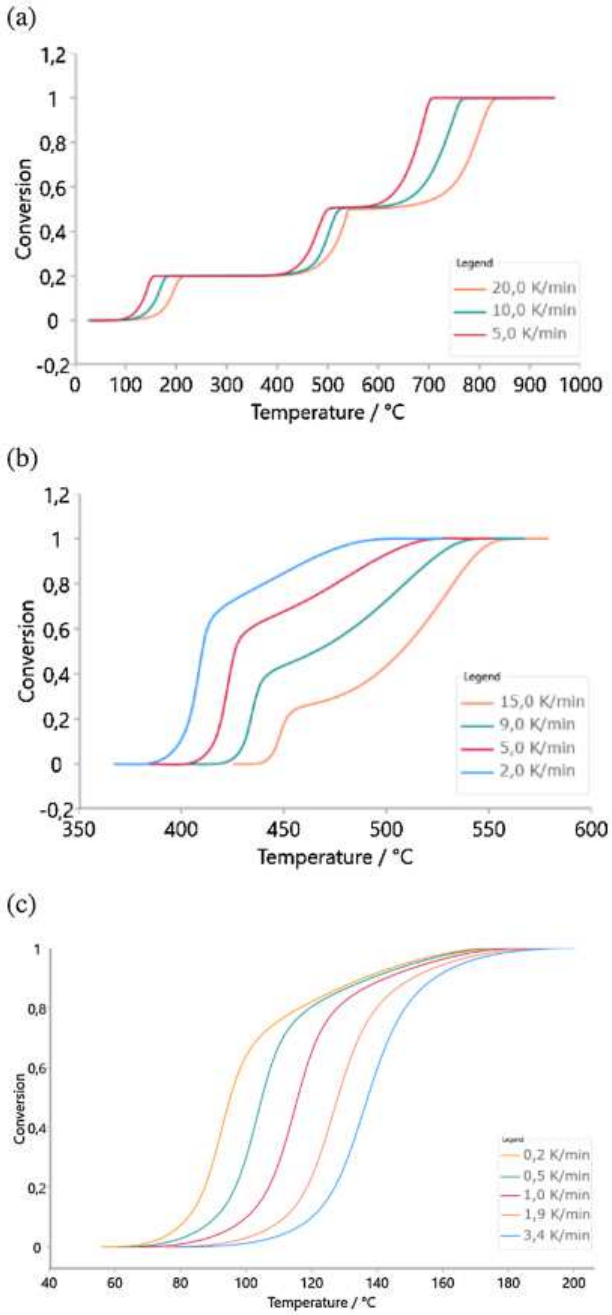

Fig. 4. Reaction mechanism changes at the same conversion (a) or at different conversion values (b,c) for different heating rates. (a) decomposition of monohydrate of calcium oxalate; (b) last two decomposition steps of ammonium paratungstate tetrahydrate, water MS traces from [18]; (c) curing with diffusion control, data from [22].

2.2 Selection of the number of steps

As mentioned in introduction, visual inspection of experimental curves often indicates that the overall reaction contains more than one step, although sometimes it may fail to reveal the multistep nature of a process. At any rate, visual inspection is more effective when applied to derivative data such as DSC or DTG. Therefore, it is recommended to calculate the first derivative curve for TGA data. The presence of several peaks and/or shoulders points to a multi-step reaction, and the number of them suggests the minimum number of reaction steps in the multi-step kinetic model. If some peak or shoulder is visible only on one experimental curve, it is necessary to carry out additional runs to determine whether this feature appears on other experimental curves under other temperature conditions. Only then it is justified to introduce

the respective step into the multi-step kinetic model. If it is known that a reaction consists of consecutive steps, but the first step is so slow that it limits the rates of other steps, the experimental curve is represented by one single peak. Kinetic analysis then demonstrates a constant activation energy, and the overall process manifests itself as a single-step reaction. If the following consecutive steps are much faster and take place immediately after the slow step, without revealing any detectable peaks or shoulders, then the kinetic parameters of these steps cannot be found from the respective experiments. The individual chemical reactions, which are not detectable as peaks or shoulders, should not be introduced into the model as consecutive or independent steps [14]. However, as mentioned in introduction, single peaks without shoulders can still appear in the case of multi-step reactions. In this case, one needs to check whether the isoconversional activation energy varies strongly and monotonically with conversion. If this is the case, and the total mass loss or heat release depends on heating rate (Figure 5), then the reaction should be described as two competing reaction steps. It should be mentioned, though, that the competing steps may have comparable contributions to the overall reaction rate so that the total mass loss or heat release may not demonstrate any significant dependence on the heating rate. In this case, discrimination between independent and competitive steps will be problematic.

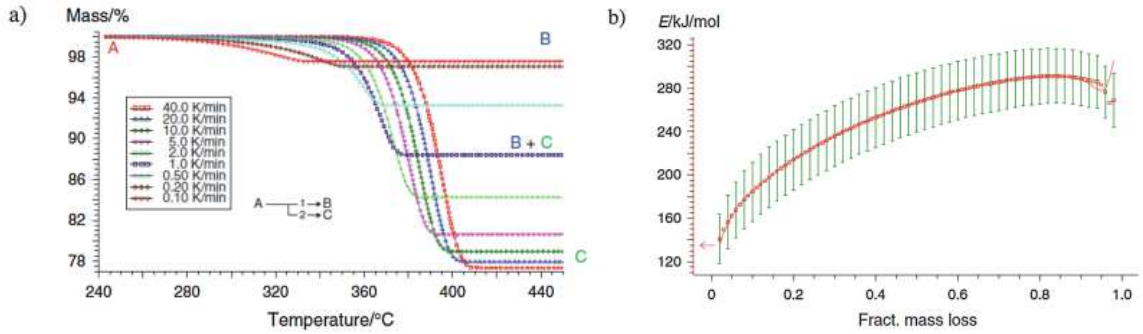

Fig. 5. Competing reactions: (a) Total effect of reaction (total mass loss) depends on heating rate for competing steps with different final products; (b) activation energy plot for these data [14]. Reproduced from Moukhina [14] under the Creative Commons Attribution License.

2.3. Construction of the multi-step kinetic model

Constructing the multi-step kinetic model should start with including main reaction steps, which exhibit the largest contribution to the total effect, i.e., the total mass loss (TGA) or the total heat (DSC). Then this rough multi-step kinetic model could be refined by adding smaller, less significant steps. Sometimes the reaction mechanism is known so that it is clear which step is responsible for which peak. In this case, the multi-step kinetic model is easily defined. However, sometimes the individual reaction steps are unknown. Then, the additional mechanistic information can be very helpful for constructing a meaningful multi-step kinetic model. For example, multi-step decomposition of an individual substance is usually a sequence of consecutive steps. If the starting material is a mixture of non-interacting components, and the final and intermediate products of each component are totally independent of the other components, then the multi-step kinetic model can consist of several independent steps or reaction pathways (i.e., sequence of steps). Here, each independent step or pathway corresponds to an individual component. If it is unknown which peak corresponds to which component, then additional experiments on individual components can help to identify the peak origins. Dependence of the total reaction effect (i.e., mass loss or heat release) on the heating rate indicates the presence of competing steps [14,15], see Figure 5.

2.4 Selection of the reaction models for individual steps

Each individual step in the multi-step kinetic model should obey a certain reaction model, $f(\alpha)$. Different reaction models give rise to different shapes of their rate peaks [1]. Therefore, if the peak is clearly visible, then reaction model can be determined by fitting the experimental data, as is done for single-step reactions [1,13,19]. However, for extensively overlapped peaks, a step may appear as a shoulder. In this case, the reaction model of the step cannot be determined by fitting. Then, independent mechanistic information should be used. For example, decomposition reactions are often of *n*th-order (F_n) or contracting geometry R_n [1] type. Reactions with the formation of crystalline products in liquid or solid amorphous phases usually follow the Avrami models, A_n. Cross-linking polymerizations are usually autocatalytic reactions, or have parallel pathways of autocatalytic and *n*th-order reactions [20]. Sometimes $f(\alpha)$ is decelerating function, and reaction rate $d\alpha/dt=-\infty$ at $\alpha=0$; in such cases, it makes sense to assume the presence of diffusion [19]. If crosslinking polymerization slows suddenly at different conversion α for slow heating rates or isothermal conditions, then this could be happening because of vitrification and diffusion control should be taken into account [21,22]. Generally, if no information about a given reaction step exists, then the step can, at least initially, be represented by the n-th order reaction model *Fn*. For reactions with acceleration [19], autocatalytic reaction models can be selected. For very sharp rate peaks for reactions with the formation of crystalline products the Avrami reaction models can be selected. If several different reaction models offer a satisfactory fit, then the model with fewer parameters should be preferred.

2.5 Comparison of alternative reaction models

Sometimes the mechanistic information about a multi-step reaction is insufficient to construct a well-defined multi-step kinetic model. Then several alternative multi-step kinetic models can be constructed. The multi-step kinetic models can differ in the number of steps, their connection, and reaction models for the individual steps. As already stated, kinetic parameters are evaluated by optimization that minimizes the *RSS* for the sum over all points and all kinetic curves. The goodness of fit by the simulated curves can be described by *RSS* as well as r^2. It should be stressed that the larger the number of the optimization parameters (e.g., the larger number of reaction steps), the better the fit, i.e., the lower *RSS* and r^2 closer to 1. Nevertheless, one should avoid overfitting, i.e., avoid introducing more steps and parameters than necessary. First, it is necessary to make sure that each step in the multi-step kinetic model is justified by available mechanistic information. In the absence of the latter, introduction of the steps into the model should be justified by experimental evidence such as detection of peaks or shoulders or significant variation of the isoconversional activation energy. An important criterion for avoiding overfitting is the F-Test [15] that can be performed on the *RSS* values. Introduction of additional kinetic parameters (or reaction steps) normally reduces *RSS*. However, such introduction is justified statistically only if a decrease in *RSS* is proved to be significant by the F-test. Otherwise, additional steps or parameters should not be introduced.

2.6 Modeling errors

Optimal kinetic parameters are evaluated by minimizing the *RSS* function, which may have several minima for multi-step reactions, and, thus, may yield different sets of the parameters depending on the starting parameters. Initial values of activation energy and pre-exponential factor could be roughly estimated from the Friedman analysis for the conversion values corresponding to each peak or shoulder. The detailed rules for selecting the starting parameters can be found in [19]. A simple example of different solutions for different initial kinetic parameters is shown in Figure 6, where a multi-peak curve can be equally well fit as the sum of positive (upward) peaks or as the sum of positive and negative (downward) peaks. If it is known from the mechanistic information that all reaction steps have positive contributions (w_i

> 0) to the overall rate, then the first solution must be kept. However, if the steps have opposing contributions, the second solution is correct.

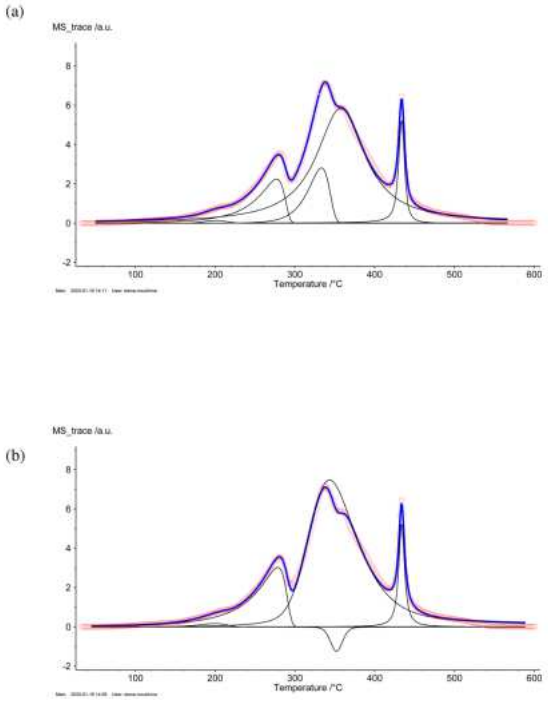

Fig. 6. Multi-step curve can be mathematically presented as the sum (blue curve) of positive peaks(a) or as the sum of positive and negative (b) peaks. Researcher should select the correct of these solutions from chemical point of view. Measured data (red circles) are the MS ammonia traces from [18]. Adapted with permission from Fait et al. [18]. Copyright 2016 Elsevier. (For interpretation of the references to colour in this figure legend, the reader is referred to the web version of this article).

2.7 Checking and interpretation of results

The optimal kinetic parameters must be critically checked for a meaning in terms of the investigated reaction.

- The contributions (weights) of all steps must be positive $w_i > 0$. Exceptions are the reactions

with steps of opposing directions, where some contributions could be negative [23]. A solution with a negative contribution must be clearly explained.

- The sum of all weights must be equal to 1

$$\sum w_i = 1 \tag{2.10}$$

If this sum is higher/lower than 1, then all contributions should be proportionally reduced/increased.

- The activation energy of a chemical reaction is normally positive that points to an increase in reaction rate with temperature. Yet, the effective activation energy could be sometimes found as a negative value for kinetic processes [24] whose rate increases with decreasing temperature as in the case of reversible reactions [25] or non-chemical processes like crystallization [26]. The reason for the negative value must be explained.
- Reaction orders are usually not higher than 3 from a chemical point of view. But some kinetic processes can be described by an n-th order reaction with very high values for n. A

solution with $n > 3$ must be either corrected or explained.

- The Avrami exponent, p, is usually not higher than 4. If a solution contains $p>4$, then it must be explained. The process is probably non-chemical.

2.8 Kinetic predictions

Kinetic analysis is based on experimental data measured within a limited range of conditions such as temperatures and heating rates. The optimal kinetic parameters evaluated for a given experimental range can be used for interpolation as well as extrapolation. Interpolation of kinetic curves within the experimental range does not typically present a problem. However, prediction of the kinetics outside the experimental range must always be done with care. For example, the kinetics evaluated experimentally at faster heating rates (5 - 40K/min) may not be applicable for slower heating rates or lower temperatures, because the reaction mechanism may change [27,28]. One of the reasons can be a phase change such as in the case of AIBN [16]. Under nonisothermal conditions (i.e., continuously rising temperature) AIBN decomposes after melting, i.e., in the liquid phase. However, under isothermal conditions the decomposition can be performed in the solid phase with different kinetic parameters. Another example is crosslinking polymerization [21], which, at fast heating proceeds completely above the glass transition temperature T_g, i.e., in the liquid state. Nevertheless, on slow heating or under isothermal conditions, the process can undergo vitrification so that its later stages take place in the glassy state and, thus, demonstrate different kinetics. In general, if it is necessary to make predictions for temperatures outside of the experimental range, one must check whether changing the temperature range associated with a transition between the phases or occurrence of new chemical reactions. If such events are present, the predictions for such temperature range can become highly inaccurate.

If the kinetics evaluated under nonisothermal conditions is intended to be used for isothermal predictions, care must be taken to confirm that the evaluated kinetics still holds outside of the experimental range [16]. As an option, one can be recommended to perform kinetic evaluations for a set of data that combines isothermal and nonisothermal runs [27]. The same is true for the temperature, because the kinetic model only works well in the temperature range in which the experiment was carried out.

3. Distributed reactivity analysis

3.1 Basics

Distributed reactivity analysis is used for complex, heterogeneous materials for which the decomposition occurs by multiple, independent, parallel reactions. Fossil organic matter [29,30, 31,32,33], biomass [34,35,36,37,38], chars from polymer decomposition [39,40,41], sintering [42], and desorption from heterogeneous sorption sites [43,44,45,46,47,48] are five applications for distributed reactivity models. The reactivity may follow a simple distribution that leads to a single curve, i.e., sigmoidal mass-loss curve (TGA) or bell-shaped mass-rate (DTG) or heat-rate (DSC) curve, or it may be one or more parts of a multi-step reaction having multiple distinct curves. Devolatilization of char from polymer decomposition is an example where the primary reaction is likely sigmoidal and the secondary reaction eliminating hydrogen and methane from the char has distributed reactivity. The fundamental assumption of distributed reactivity models is that the individual reactive moieties do not interact with each other, which provides the basis for the independent parallel reaction construction [39]. In continuous form, it is given by convolving over $D(E)$, the mathematical distribution function of E:

$$\frac{d\alpha}{dt} = \int_0^{\infty} k(E, T) \exp\left[-\int_0^t k(E, T) dt \right] D(E)\, \mathrm{d}E \tag{3.1}$$

for first-order reactions and

$$\frac{d\alpha}{dt} = \int_0^\infty k(E,\,T)\left[1-(1-n)\int_0^t k(E,\,T)dt\right]^{n/(1-n)} D(E)\,\mathrm{d}E \tag{3.2}$$

for *n*th-order reactions.

The discrete form is a simple summation and easier to understand:

$$\frac{d\alpha}{dt} = \sum_i w_i k_i(E_i,\,T) f_i(\alpha_i) \tag{3.3}$$

where

$$\alpha = \sum_i w_i \alpha_i \tag{3.4}$$

and w_i are the weighting coefficients for the individual reactions and sum to unity. In this case, $f_i(\alpha_i)$ can easily be any single-step reaction model. The parallel reactions can have the same preexponential factor, or the preexponential factor can be some function of the activation energy. The function is usually

$$\ln(A_i) = a + bE_i \tag{3.5}$$

where *a* and *b* are simply constants. This extension from a single preexponential factor is usually unnecessary for practical purposes, even for relatively large extrapolations in temperature [39]. It may be helpful for theoretical interpretation, but global models such as distributed reactivity have so many approximations that any theoretical interpretation is qualitative at best.

3.2 Distribution forms

The reactivity distribution can be either an analytical distribution or an arbitrary discrete distribution—both approaches have been used for more than 50 years. Although some have tried direct integration of the continuous distribution and various mathematical approximations thereto [49], it is far simpler and computationally faster to convert the continuous distribution to a closely spaced, discrete distribution and integrate the independent reactions separately [39]. Reaction spacing of 4 kJ/mol gives excellent numerical accuracy for the assumption of parallel first-order reactions, which is the most common method. However, parallel *n*th-order reactions (*n*=1.5 or 2.0) can be spaced further apart for the same numerical accuracy with less computational time [50]. The discrete energy distribution has arbitrary weighing factors for the individual reactions with different activation energies as shown in eq. 3.3. It was first used in a forward sense for coal pyrolysis [29]. The first approach to optimize by direct non-linear regression [51] was very slow, but an iterative linear-constrained nonlinear regression method soon followed [52]. This approach usually uses a common preexponential factor for all reaction channels, but some commercial programs allow it to have the compensation form of eq. 3.5. This approach is by far the most common one to derive kinetic models for simulating petroleum formation in geological time for petroleum exploration.

A variety of analytical distributions have been used, most often a Gaussian distribution [30] but also Weibull [53,54,55], gamma [33,56,57], logistic [58,59], and pseudo-*n*th-order distributions [39]. It might be surprising to call the latter a distributed reactivity model, but it is mathematically similar to one limit of the gamma distribution and power-law temporal models, which are similar to a distribution of preexponential factors [33,39]. Also important is that this construct is fundamentally different from the concentration dependence of bimolecular reactions in solutions, which is why it is properly called a pseudo *n*th-order model.

The distribution equations are shown in Table 1, and examples of distributions for various parameter values are shown in Figure 7. The Gaussian and common logistic distributions have the advantage and disadvantage of being a simple shape. There is only one parameter, which makes them easy to optimize, but there is no reason to expect that an activation energy

distribution should be symmetric. This can be rectified by using pseudo-*n*th-order reactions in concert with those distributions, which provides the ability to change the asymmetry. The gamma, Weibull, and asymmetric logistic models already contain two parameters that, in effect, control the width and asymmetry of the distribution. In fact, the gamma and Weibull distributions are mathematically identical for some sets of parameters. But these models are also so diverse in the available distribution shapes that convergence is more challenging.

Table 1
Probability Distribution Functions used for modeling distributed reactivity.

Distribution	Equation
Weibull	$D(E) = \frac{\kappa}{\lambda}(\frac{E-E_0}{\lambda})^{\kappa-1}\exp[-(\frac{E-E_0}{\lambda})^{\kappa}]$
Gamma	$D(E) = \frac{\theta^{\varphi}}{\Gamma(\varphi)}(E-E_0)^{(\varphi-1)}\exp(-\theta(E-E_0))$
Gaussian	$D(E) = \frac{1}{\sigma\sqrt{2\pi}}\exp[-\frac{1}{2}\left(\frac{E-E_0}{\sigma}\right)^2]$
Symmetric logistic	$D(E) = \frac{e^{-(E-E_0)/s}}{s[1+e^{-(E-E_0)/s}]^2}$
Asymmetric logistic	$D(E) = \frac{e^{-(E-E_0)/s}}{s[1+\tau e^{-(E-E_0)/s}]^{\frac{1}{\tau}+1}}$

The logistic model situation is more complicated, in that logistic functions have been used in fundamentally different modeling approaches. Part of the difference is whether the logistic function is considered to be a probability distribution function for E as shown in Table 1 or a solution to α versus t. For the latter, recall that the logistic function is the solution to the basic autocatalytic reaction with E equal for initiation and growth reactions [60]. The logistic model can be extended in two ways—in an extended Prout-Tompkins (truncated Šesták-Berggren) form, where a growth parameter m is introduced as well as the reaction order n:

$$\frac{d\alpha}{dt} = k(T)\alpha^m(1-\alpha)^n \tag{3.6}$$

The parameter m is zero for an nth-order reaction, and m=n=1 for the regular Prout-Tompkins limit. The reaction profile gets narrower at a constant heating rate as m increases, as is typical for nucleation-growth reactions. But when m<0, which has no physical meaning, the reaction profile is also broader than a first-order reaction, which mimics an activation energy distribution. Using both m and n can modify the shape of the reaction profile, hence the implicit activation energy distribution, also. A much better way to use the logistic function for distributed reactivity is shown in Table 1. In this case, the abscissa of the distribution function is activation energy, not time, and the function has been transformed linearly so that the center of the distribution is the mean activation energy. The logistic distribution is symmetric, so Cai et al. [59] explicitly considered the convolution over a pseudo-nth-order reaction to enable control of the reaction profile asymmetry as well as width.

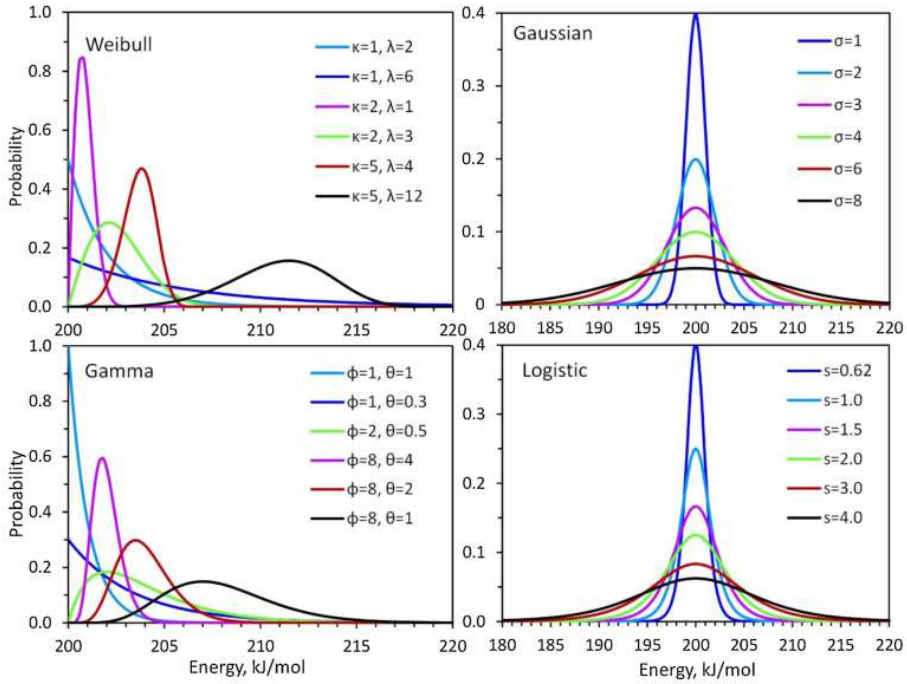

Fig. 7. Probability Distribution Functions used for modeling continuous activation energy distributions. The Weibull and gamma distributions are quite flexible, and the Gaussian and symmetric logistic models are limited. The asymmetric logistic model (not shown) can introduce some skewness to the activation energy distribution.

Alternatively, one can introduce an asymmetry factor directly into the logistic distribution to create an asymmetric reactivity distribution. On can apply an asymmetric logistic function directly to the α versus time curve [61], but it has no advantage over eq. 3.6 [62]. Even so, the generalized equation, which is shown in Table 1 but not in Figure 7, can be used as an alternative to convolving *n*th-order reactions with an energy distribution to achieve an asymmetric reactivity distribution. No one has done this yet to our knowledge.

3.3 Optimization methods

After choosing a distributed reactivity model, optimizing that model requires both a mathematical definition of the best fit of the model to the data and a mathematical way of achieving it. The first aspect requires some sort of comparison between calculated and measured observables. This comparison can be a visual comparison, an estimation from a correlation between model parameters and some simple characteristics of the reaction profile, or a full mathematical optimization. We like to think that the latter can derive the best fit, but even then, there are different ways to define what is best. This definition of best is coded into what is called the objective function, and the purpose of the nonlinear regression is to minimize that objective function. But even what is deemed objective is subjective. The most common quantity to be minimized is the residual sum of squares (RSS) between the calculated and measured reaction property as a function of time or temperature. Given that each point has a time and temperature, they are equivalent. This leads to the relation

$$Best = minimum\,[\Sigma_i(x_{i,calc} - x_{i,meas})^2] \quad (3.7)$$

However, that objective function is not uniquely the best. For example, one could minimize the difference in both the *x* and *y* directions,

$$Best = minimum\,[\Sigma_i((x_{i,calc} - x_{i,meas})/x_{max})^2 + \Sigma_i((y_{i,calc} - y_{i,meas})/y_{max})^2] \quad (3.8)$$

where x_{max} and y_{max} are normalization factors equal to the maximum values of *x* and *y* in the experiment. Alternatively, one could have a percentage or some other functional difference between calculated and measured values that relates to the character of the data or the

application.
For example,

$$Best = \ minimum\,[\Sigma_i(\ln(x_{i,calc}) - \ln(x_{i,meas}))^2] \tag{3.9}$$

more heavily weights the smaller values near the beginning and end of a nonisothermal rate curve.
In addition, one could minimize the chosen objective function for reaction rates, fractions reacted, or both simultaneously (again using normalization factors when rates and fractions reacted are minimized simultaneously). Experience suggests that when the reaction-rate baseline is known well and the reaction extent approaches complete conversion, simultaneous minimization of rates and fractions reacted gives more robust chemical kinetic models, because rates and fractions reacted are sensitive to different details of the reaction.
Next, the collection of experiments being used in the optimization usually have a different number of points—should the experiments be weighted equally or inversely related to the number of points? This is an important issue, because thermal analysts usually collect data at constant time intervals regardless of heating rate. Again, experience suggests that if all experiments have hundreds of points, unless there is some reason to suspect any given experiment, all experiments should be weighted equally by dividing the residuals by the number of data points to prevent undue influence of any experiment that has more points but not truly more information.
The last question on this aspect is if one has multiple observables—two or more of mass, heat, evolved gas composition, etc.—how does one construct the proper multicomponent model and objective function? However, this task is normally outside the scope of thermal analysis and is not considered here. The second aspect is how to minimize the objective function. The more complex the function and parameters to be optimized, the more complex the minimization surface and the likelihood that one will find a local minimum and not the global minimum. Some minimization methods are more robust than others to avoid this problem. The standard for nonlinear regression for many years has been the Levenberg-Marquardt algorithm, which is a damped least-squares method that interpolates between the Gauss-Newton algorithm and method of gradient descent. Very simply, the computer evaluates the error of the supplied guesses and migrates towards a minimum that meets a specified goodness of fit. Its success depends on the quality of the initial guesses, and it is not a robust method for optimizing many parameters simultaneously. There are many other methods with various strengths and weaknesses. Genetic algorithms and artificial neural networks can be very efficient for this purpose [63]. Recently, Genetic Algorithm, Simulated Annealing, Grid Search, Shuffled Complex Evolution, Stochastic Hill Climbing, Particle Swarm Optimization, and a few others were evaluated by Purnomo et al. [64] within the context of optimizing biomass pyrolysis kinetics. The best method depended on the nature of the objective function and the relative importance of computer time and accuracy. The overall best method was said to be Shuffled Complex Evolution, but they did not consider distributed reactivity models. Reaching a robust solution is enhanced by using a sequential combination of methods. Some have found that a sequential combination of methods for the early and late stages of optimization works better than using a single optimization method [65]. Another approach is to use simple methods, such as isoconversional analysis and Kissinger analysis combined with simple correlations to provide better initial parameter values for the nonlinear regression [32,52]. Either approach can work. One final issue is that optimization of the discrete *E*-distribution model works differently.
Iterative nonlinear-linear regression separately refines the preexponential factor and the respective range of activation energies that span the data space. The linear regression optimizes the weighing factors of individual reactions at evenly spaced activation energies for the current preexponential factor. Although it seems that many parameters are being optimized, the

relationship among them makes that easily possible. One subtlety is that differences in the reaction space covered by different experiments sometimes leads to spurious weighting on the end of the energy distribution. This is mitigated by simultaneous regression of both rates and fractions reacted, which is possible when the reaction goes nearly to completion.

3.4 Source-sink and quench-reheat issues

Many materials needing a distributed reaction model also have what might be considered as primary and secondary reactions. In other words, the original material breaks down into a combination of volatile and non-volatile products, and the non-volatile products break down by substantially different chemical kinetics. The non-volatile products usually fall into the category of what one might call char or coke, and the breakdown of char or coke is always characterized by distributed reactivity even if the primary reaction is not. Most people approach this primary-secondary reaction issue by assuming they are independent, parallel processes. This approach often works well, but when the yield of char depends on heating rate or pressure or some other variable, which is common, it breaks down. Of course, this can be fixed only by incorporating a competitive reaction component to the primary reaction, whereby the ratio of volatile to non-volatile products from the primary reaction depends on conditions. This construct is more common in chemical reaction engineering than in thermal analysis. The situation can become more complicated if one considers that the nature of the distributed reactivity of the secondary material depends on the conditions of its formation. Furthermore, if both the primary and secondary reactions have distributed reactivity, one must postulate or demonstrate how the more labile and refractory components of the primary reaction populate the reactivity channels of the secondary reaction. Usually one assumes that each reactive component in the primary reactivity distribution contributes equally to the full reactivity distribution of the secondary reaction. The pseudo-*n*th-order reaction approach is not suitable for materials generated during the reaction (reaction intermediates). Recall that the pseudo nature is based on the fraction reacted of an initial material, and that fraction is undefined when it is both generated and consumed in a reaction. Consequently, only a distribution of activation energies is appropriate when sequential reactions are considered.

Distributed reactivity materials have the characteristic that when heated and partially reacted, then cooled and reheated, their reaction characteristics will be different than for the initial heating. Basically, the more labile material has already been consumed, so higher temperatures are needed to achieve the initial reaction rates. This is different than for a first-order reaction, which is independent of thermal history, and it is opposite to nucleation-growth and initiation-propagation reaction systems, where the reactivity upon reheating is greater than during the first heating. Pseudo *n*th-order reactions can model this characteristic if they are present at initial time, but activation energy distribution models can model this characteristic whether they are initially present or generated by prior reactions.

3.5 Examples

Two examples are presented to demonstrate some aspects involved with distributed reactivity. The first is pyrolysis of a bituminous coal [39], and the other is pyrolysis of poly(vinyl chloride) (PVC) [66]. As is typical, both involve a primary pyrolysis step that produces a char, followed by secondary pyrolysis of that char. In both cases, pyrolysis of the char is characterized by reactivity distributions. The difference between the two cases is that the primary step for bituminous coal is also characterized by distributed reactivity while the primary step for PVC is characterized by sigmoidal (nucleation-growth or initiation-propagation) kinetics.

Table 2 and Figure 8 show the analysis results for bituminous coal. Both isoconversional analysis (Friedman) and the shift in T_p versus heating rate (Kissinger) give a

mean activation energy about 230 kJ/mol. Although not shown, the isoconversional analysis found *A* and *E* to increase substantially over the course of the reaction. Comparing the reaction profile width to that calculated from the Kissinger *A* and *E* values suggests a reactivity distribution comparable to 3-4% of the mean activation energy, but it is clear by simply looking at the reaction profiles that a single symmetric reactivity distribution is not adequate. This is why the *n*th-order reaction fit is better than a Gaussian *E*-distribution. Two Gaussians are needed for an acceptable fit, but the Discrete *E*–distribution model is significantly better still. Simultaneously fitting to reaction rates and fractions reacted to the Discrete *E* model gives an arguably better result, given that the sum of residuals from rates and fractions reacted are less than when fitting to only one or the other. In a more general sense, the line describing the tradeoff between fitting the rates and fractions reacted (i.e., two distinct objective functions) is called the Pareto front [67]. The Pareto front quantifies the notion that the definition of "best fit" involves some subjectivity in how one defines the objective function. Table 3 shows analysis results for a variety of distributed reactivity models for PVC. The models are visually equivalent (comparable to Figure 8), although slightly better fits (lower RSS) are obtained if non-unity reaction order is allowed for the initial nucleation-growth step. One should consider, of course, whether such an improvement is justified statistically [68], but the full nature of that question depends on how the kinetic model will be used. For char pyrolysis, equally good fits are obtained using *n*, σ, or *m* as the reactivity distribution parameter. The only issue is that the negative value of *m* for the second peak in Table 3 has a dubious physical meaning When positive, *m* is growth dimensionality or autocatalytic strength; it becomes a self-poisoning feature when negative.

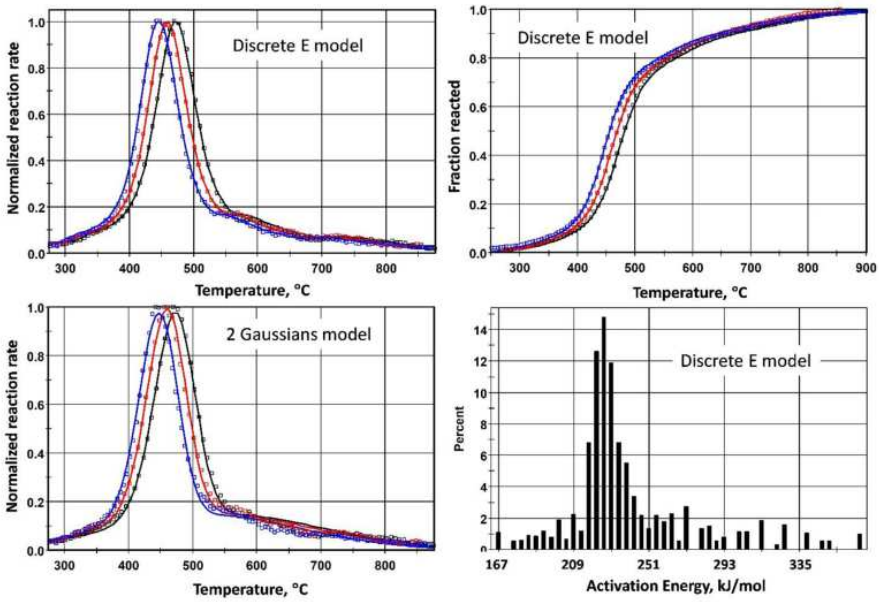

Fig. 8. Fits of two distributed reaction models to pyrolysis of bituminous coal at heating rates of 5, 10, and 20°C/min. In this case, the Discrete *E*-distribution model was fitted simultaneously to rates and fractions reacted. The fit of two Gaussians to the data is almost indistinguishable from the Discrete *E*-distribution model for fraction reacted, but small differences are evident for reaction rates.

Table 2
Distributed reactivity kinetic analysis results for mass loss from bituminous coal heated at 5, 10, and 20 °C/min. Except for the last two lines, various models were fitted simultaneously to fractions reacted data (I) at all heating rates by nonlinear regression. The last line gives results for the Discrete *E*-distribution model fitted simultaneously to fractions reacted (I) and reaction rates (R).

Kinetic model	*E* type	*E*, kJ/mol	ln(A/s^{-1})	rxn order, n	Gaussian σ	RSS, I	RSS, R
Friedman	E at $\alpha = 0.5$	247	34.1	1	0	—	—
Kissinger	E for T_{max}	215	30.5	1	0	—	—
*n*th-order	E	205	29.7	5.0	0	0.196	2.82
Gaussian	Mean E	257	35.9	1	11.3	0.799	6.09
Two Gaussian	Mean E's	233, 257	33.2	1	3.1,2.0	0.024	0.104
Discrete E, I	Primary E	247	35.7	1	0	0.009	0.051
Discrete E, R	Primary E	222	31.6	1	0	0.035	0.020
Discrete E, I&R	Primary E	226	32.1	1	0	0.015	0.024

A characteristic of distributed reactivity situations is that partial heating causes the remaining material to be more refractory [69]. This characteristic is modeled in Figure 9 for PVC using parameters given in Table 3. The shift in the maximum rate of char devolatilization after quench is due to elimination of the more labile components, not conversion of any material to more refractory components, even though the latter is possible in reactivity. The pseudo-*n*th order and Gaussian *E*-distribution models probably describe this shift in the temperature of maximum rate more accurately, although there are no systematic studies of this effect for polymers.

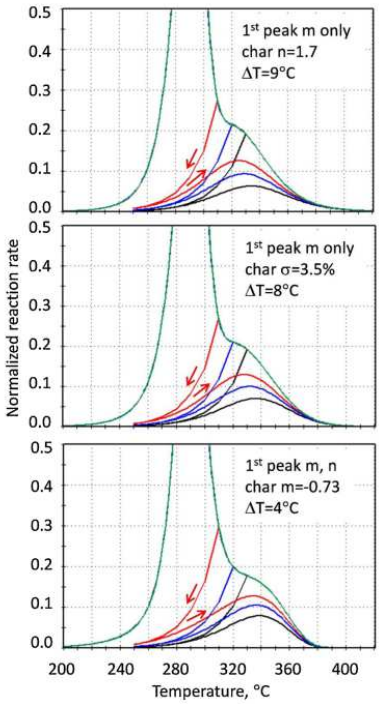

Fig. 9. Reaction trajectories for three PVC reactivity distribution models upon heating at 10°C/min to incomplete reaction at 310, 320, and 330°C then reheating through complete reaction. Due to partial reaction of the char before quench, the subsequent maximum rate of its devolatilization shifts to higher temperature by an amount that depends on the initial heating schedule, as indicated by ΔT.

Table 3
Kinetic analysis results for mass loss from poly(vinyl chloride) heated at 2.5, 5, 10, and 15 °C/min. The reactivity distribution is characterized by a nucleation-growth model (NG) followed by a distributed reactivity model for the generated char. All non-linear regression models were simultaneously optimized on fractions reacted and reaction rates, using an initiation reaction 1% as fast as the propagation reaction in the NG model. P1 and P2 are the two parameters optimized in each specific char model.

Kinetic model	f_1	E_1, kJ/mol	$\ln(A_1/s^{-1})$	m_1	n_1	E_2, kJ/mol	$\ln(A_2/s^{-1})$	P1	P2	RSS, I	RSS, R
Friedman	—	128.5	22.1								
Kissinger	—	133.6	23.8								
								σ	n		
NG-Gaussian	0.60	129.7	23.8	0.67	1.00	152.6	26.0	3.7	1.00	0.020	0.110
NG-*n*th	0.62	129.9	23.9	0.65	1.00	146.7	25.0	0.0	1.69	0.021	0.109
NG-Gaussian *n*th	0.61	129.0	23.7	0.67	1.00	151,4	26.0	2.3	1.52	0.020	0.108
NG-Gaussian *n*th	0.61	130.2	24.2	0.76	1.24	151.3	25.5	4.4	0.56	0.018	0.078
								m	n		
NG-logistic	0.63	128.7	23.6	0.66	1.00	146.0	24.8	0.00	1.67	0.020	0.112
NG-logistic	0.66	130.1	24.2	0.78	1.37	151.73	24.8	−0.73	1.00	0.020	0.080
NG-logistic	0.66	130.0	24.1	0.76	1.31	155.4	26.0	−0.51	1.30	0.018	0.071

4. Isoconversional analysis

4.1 Basics

Isoconversional methods permit estimating the activation energy as a function of conversion. As explained in introduction, for a single-step process E_α should be practically constant, i.e., should not demonstrate any significant variation with α. When variation in E_α exceeds 10–20 % of the average E_α, the process should be considered as multi-step. All isoconversional methods take their origin in eq. 1.2, which is derived under the assumption of the single-step kinetics (eq. 1.1). Although this assumption does not hold strictly for multi-step kinetics, it can still be used as a reasonable approximation. More specifically, at constant α and within a relatively narrow range of temperatures related to this α, multi-step kinetics can be approximated as a single-step one [70]. This approximation permits extending the application area of isoconversional methods to analysis of multi-step reactions. It means that an experimentally found dependence of E_α on α allows one not only to detect multi-step kinetics. It also enables estimating kinetic parameters of individual steps. The principle is simple. For example, in eq. 1.5 the left hand side, i.e., the variable E_α can be determined experimentally. The right hand side is the variable $E\alpha$ defined theoretically, i.e., from a multi-step kinetic model. Then, the parameters of the latter can be estimated as the values that minimize the deviation between the theoretical and experimental $E\alpha$ dependencies. As seen from eq. 1.5, E_α generally depends on both α and T. Therefore, both dependencies should be determined for performing minimization and estimating the kinetic parameters. The dependence of E_α on α is determined directly by an isoconversional method. Since the parameters of a multi-step model are estimated from the E_α values, the accuracy of E_α affects the accuracy of the resulting parameters. Thus, one should use the most accurate isoconversional methods. This issue has been addressed in the previous recommendations [1] and it concerns primarily the integral methods. The problem is that the most popular methods such as those of Ozawa [71] and Flynn-Wall [72,73], Kissinger-Akahira-Sunose [74], and Starink [75] are rigid [70,76] integral methods, meaning that their basic equations arise from rigid integration limits from 0 to a given value of α. This approach gives rise to a systematic error in the E_α values, when E_α demonstrates a significant variation with α [1,77,78]. Another problem with the rigid integral methods is that they are not applicable to the processes occurring on cooling [70,76]. This problem as well as the afore-mentioned systematic error is eliminated by using flexible [70,76] integral methods. These are the methods that utilize integration over small segments of α [77,79,80,81,82,83,84,85,86,87,88,89]. The flexible methods can be applied to the processes that occur on cooling such as crystallization of a polymer melt [26], gelation of a polymer solution [90], morphological solid-solid transition [91], crystallization of a salt from a solution [92], as well as thermal decomposition [93] and crosslinking polymerization [94] taking place during continuous cooling. Equally, one can eliminate the systematic error in $E\alpha$ and treat processes occurring on cooling by employing the differential method of Friedman [95] or similar techniques [96]. Therefore, when the $E\alpha$ dependence is intended for estimating the kinetic parameters of a model, it is recommended that

the E_α values be determined by either a differential or flexible integral method. The accuracy of estimated kinetic parameters is usually checked by using them to simulate kinetic curves and comparing these curves against the ones actually measured. For model-fitting techniques, the simulations are done by using full kinetic triplets. The same approach can be used for isoconversional methods [1]. However, for isoconversional methods it is also possible to perform such simulations by using the evaluated dependence of $E\alpha$ on α, without evaluating the two other components of the kinetic triplet. The respective equations for isothermal and nonisothermal simulations were derived earlier [97,98]. It should be noted that these equations were originally designed for the cases when E_α does not vary significantly with α. For accurate simulation of processes with a significant variation in $E\alpha$ integration in the respective equations should be performed over small segments of α as explained elsewhere [1,76]. The dependence of E_α on T is determined from the experimental dependence of E_α on α. In an isoconversional method, the E_α on α dependence is evaluated by using multiple temperature programs such as heating or cooling at multiple rates of temperature change. Under these conditions, the same α is reached at different temperatures under different temperature programs.
Taking the average value of these temperatures and substituting it for α in the dependence of E_α on α yields the dependence of E_α on T. As already stated, E_α generally depends on both α and T, i.e., $E_\alpha=E(\alpha,T)$. Therefore, the parameters of a model are estimated by minimizing the deviation between the model and experimental E_α values as a function of two variables, α and T. However, there are practically important cases when the model parameters can be determined by fitting the $E\alpha$ vs T dependence alone. In principle, this approach can be applied to any multi-step process whose isoconversional activation energy can be obtained in the form of an algebraic expression (cf., eq. 1.5). In the following sections we consider two specific examples that are representative of the two types of fits. These examples are nucleation driven phase transitions (fitting $E\alpha$ vs T) and crosslinking polymerization (fitting E_α vs both α and T).

4.2 Nucleation kinetics

The temperature dependence of the nucleation rate is generally described well by the Turnbull and Fisher model [99]:

$$w(T) = w_0 \exp\left(\frac{-E_D}{RT}\right)\exp\left(\frac{-\Delta G^*}{RT}\right) \tag{4.1}$$

where w_0 is the preexponential factor, ΔG^* is the free energy barrier to nucleation and ED is the activation energy of diffusion. This is the model that combines two steps, the formation of a new phase nucleus and diffusion of molecules across the phase boundary. The ΔG^* value is positive but decreases quickly when temperature deviates from its equilibrium value. For crystallization, under the assumption of a spherical nucleus, ΔG^* decreases with decreasing T as follows [76]:

$$\Delta G^* = \frac{16\pi\sigma^3 T_m^2}{3(\Delta H_m)^2(\Delta T)^2} = \frac{C}{(\Delta T)^2} \tag{4.2}$$

where σ is the surface energy, ΔH_m is the melting enthalpy, $\Delta T = T_m - T$ is the supercooling, i.e., the deviation from the equilibrium melting temperature, T_m, and C is the constant that collects all parameters that are practically independent of temperature. Substituting the right hand side of eq. 4.2 for ΔG^* in eq. 4.1 and then replacing $k(T)$ in eq. 1.1 with $w(T)$ from eq. 4.1, followed by taking the isoconversional derivative yields [76]:

$$E_\alpha \equiv E(T) = E_D - C\left[\frac{2T}{(\Delta T)^3} - \frac{1}{(\Delta T)^2}\right] \tag{4.3}$$

This equation describes the theoretical temperature dependence of E_α. The experimental dependence is obtained by applying an isoconversional method to the actual data. Fitting the theoretical dependence to the experimental one affords estimating the model parameters, ED and C. The parameter C can then be inserted into eq. 4.2 to determine the value of ΔG^* as a function of temperature. Eq. 4.1 can also be adjusted to other phase transitions such as melting [100], gelation [101], and solid-solid transition [91].

Note that in eq. 4.1 the exponential terms containing E_D and ΔG^* have opposite dependencies on temperature. When temperature increases, the exponential term containing ED increases, whereas the exponential term containing ΔG^* decreases. As a result, the product of these two exponential terms passes through a maximum. For this reason, the temperature dependence of the overall nucleation rate (eq. 4.1) also passes through a maximum. When a transition occurs on cooling and not far from equilibrium the temperature dependence of its rate is determined by the exponential term containing ΔG^*. Thus the rate increases with decreasing temperature. This is anti-Arrhenian behavior that manifests itself via negative values of the isoconversional activation energy. If the same transition occurs far from equilibrium, i.e., at much larger supercoolings, the temperature dependence of its rate becomes determined by the exponential term containing E_D. Then the rate decreases with decreasing temperature, which is the regular Arrhenian behavior characterized by positive values of the isoconversional activation energy. Crystallization from the glassy state usually occurs at much larger supercooling than crystallization from the melted state. This is why the former process normally yields positive $E\alpha$ values and that latter the negative ones. For transitions that occur on heating, i.e., by superheating with respect to equilibrium temperature, both terms in eq. 4.1 give rise to the Arrhenian behavior. Thus, the rate of such transitions increases with increasing temperature so that the $E\alpha$ values are positive. Examples of such processes are melting [100] or solid-solid transitions [12]. A detailed discussion of these phenomena and respective $E\alpha$ vs T dependencies is provided elsewhere [76].

4.3 Crystallization kinetics of polymers

Nowadays, the experimentally derived dependencies of E_α on T are commonly used for estimating of the Hoffman-Lauritzen parameters for crystallization of polymers [3,102]. The Hoffman–Lauritzen theory [103,104] describes the temperature dependence of the growth rate G measured microscopically by eq. 4.4:

$$G = G_0 \exp\left(\frac{-U^*}{R(T - T_\infty)}\right)\exp\left(\frac{-K_g}{T\Delta T f}\right) \tag{4.4}$$

where G_0 is the pre-exponential factor, U^* is the activation energy of molecular diffusion across the interfacial boundary between the melt and crystals, K_g corresponds to the energy barrier for the formation of critical size nucleus, $\Delta T = T_m - T$ is the supercooling, T_m is the equilibrium melting temperature (typically evaluated by the Hoffman–Weeks procedure), $f = 2T/(T_m + T)$ is the correction factor, T_∞ is a temperature where motion associated with viscous flow ceases that is taken as 30 K below the glass transition temperature T_g, i.e. $T_\infty = T_g$ -30 K. Adjusting eq. 4.4 to the volumetric crystallization rate measured by DSC followed by taking the isoconversional derivative gives rise to the theoretical temperature dependence of the effective activation energy [105]:

$$E_\alpha \equiv E(T) = U^*\frac{T^2}{(T - T_\infty)^2} + K_g R\frac{T_m^2 - T^2 - T_m T}{(T_m - T)^2 T} \tag{4.5}$$

The experimental dependence of E_α on T is obtained from the dependence of E_α on α determined by applying an isoconversional method to the actual DSC data. As explained earlier, the procedure involves replacing each value of α with the mean temperature, $\overline{T_\alpha}$ related to this α.

The procedure is illustrated in Figure 10. It should be noted that the Hoffman-Lauritzen theory takes its origin in the Turnbull-Fisher model and, thus, shares common traits with the latter. First, the rate G passes through a maximum at a characteristic temperature, T_{max}. Second, the values of E_α estimated on cooling from the melted state are negative, whereas the ones estimated on heating from the glassy state are positive. The change in the sign of E_α is seen clearly (Figure 10) for the melt and glass crystallization of poly(ethylene 2,5-furandicarboxylate). A general discussion of the phenomenon is given elsewhere [106].

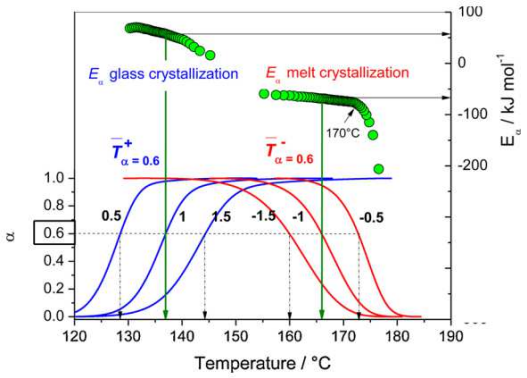

Fig. 10. E_α vs. T dependencies for the glass and melt crystallization of poly(ethylene 2,5-furandicarboxylate) (circles). The E_α vs T dependence is determined by replacing α with the average value of T. For example, for α = 0.6 is replaced with $\overline{T_\alpha}$=0.6. For the glass crystallization, it is calculated as the average of the three values of T 0.6 determined respectively from the α vs T curves obtained respectively at the three heating rates: 0.5, 1, and 1.5 K min^{-1} (blue curves). For the melt crystallization, T =0.6 is determined by averaging the three values of T 0.6 and obtained respectively from the α vs T curves measured at the three cooling rates: -0.5, -1, and -1.5 K min^{-1} (red curves). Adapted with permission from Codou et al. [108] Copyright 2014 Wiley-VCH. (For interpretation of the references to colour in this figure legend, the reader is referred to the web version of this article).

Once the experimental dependence of E_α vs T is determined, the parameters U^* and K_g are evaluated by a nonlinear fitting of eq. 4.5 as presented in Figure 11. In this approach both parameters are adjustable. Note that eq. 4.4 can be reduced to a linear form [107] assuming that U^*= 6.3 kJ mol^{-1}, which is sometimes treated as the universal value. However, one should be warned against such practice because when treated as adjustable parameter, the values of U^* are known to deviate by more than 100% from 6.3 kJ mol^{-1}.

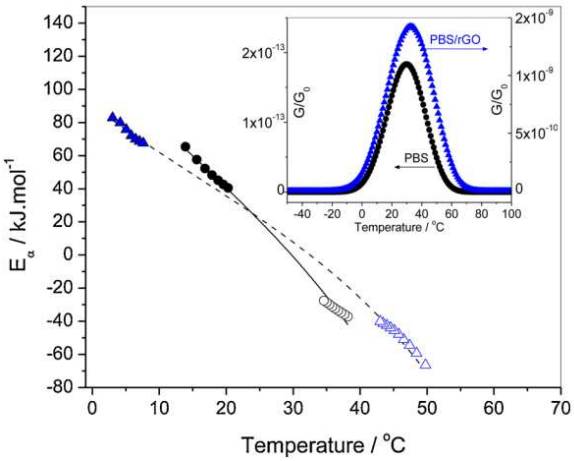

Fig. 11. Fitting E_α vs T dependencies for glass (solid symbols) and melt (open symbols) crystallization data for poly(butylene succinate) (circles) and poly (butylene succinate) graphene oxide system (triangles). Inset shows the temperature dependence of G/G_0 computed using the Hoffman– Lauritzen parameters. Adapted with permission from Bosq et al. [109]. Copyright 2017 ACS.

When fitting eq. 4.5 to the E_α vs T data one should be watchful of breakpoints. For example, a breakpoint is seen at 170°C for the melt crystallization data presented in Figure 10. A common source of this is a change in the crystallization mechanism. According to the Hofman-Lauritzen theory, with increasing the supercooling the mechanism can switch successively from regime I to regime II and regime III. The first change (I to II) results in 2 times decrease of the K_g value, whereas the second change (II to III) causes K_g to increase 2 times. When a breakpoint occurs, the segments of the E_α vs T before and after the breakpoint should be fitted separately to determine U^* and K_g for the respective regimes of crystallization. The regime III occurs at very large supercoolings that are typically accomplished on heating from the glassy state. A transition from regime I to II is commonly encountered on cooling of the melts. The breakpoint at 170°C seen in Figure 10. is an example of such transition, which is confirmed independently by X-ray methods [108]. An overview of other examples is provided elsewhere [102]. When the melt and glass crystallization occur respectively in regimes I and III, the K_g value does not change so that the melt and glass crystallization data can be fitted together by one eq. 4.5. Figure 11 illustrates this type of fits for crystallization of poly(butylene succinate) systems [109]. Doing so has an advantage of improving the precision and accuracy of the K_g and U^* values [106]. Overall, the values of K_g and U^* determined from the E_α vs T dependence agree well with the values obtained by the direct application of eq. 4.4 to the microscopy measurements [102,3]. Being fundamental parameters of crystallization, the values of K_g and U^* are of importance by themselves. In addition, they can be used to determine another important parameter, T_{max}, which is the temperature of the maximum crystal growth rate. To determine the absolute value of the maximum rate according to eq. 4.4 one needs to know the value of the pre-exponential factor G_0 in addition to K_g and U^*. However, because G_0 is a constant, the plot of G/G_0 vs T has the same position of the maximum as the plot of G vs T. The former is readily obtained by substituting Kg and U^* into eq. 4.4 [108,109,110,111]. Plots constructed in such way are displayed in inset of Figure 11. The T_{max} values determined from the values of K_g and U^* generally are in good accordance with the T_{max} values measured experimentally [108] and thus can be used for estimating such values. This is especially of importance in the case of fast crystallizing polymers such as polytetrafluoroethylene, for which the T_{max} region may not be accessible even when using very fast cooling rates [110].

It should be noted that the preexponential factor (G_0) in eq. 4.4 cannot be determined via isoconversional analysis of DSC data. The reason is that G_0 is measured in units of the linear rate, i.e., m s^{-1} which is impossible to determine without knowing the surface area of the growing crystalline phase. For this very reason, the knowledge of K_g and U^* is insufficient to simulate the growth rate, G. However, these parameters can be used successfully to simulate the overall rate of crystallization $d\alpha/dt$ or the heat flow. The respective numerical procedure is explained in detail elsewhere [112].

4.4 Kinetics of crosslinking polymerization

As far as analyzing the experimental values of E_α as a function of two variables, α and T, the most practically important application involves the kinetics of crosslinking polymerization (i.e., curing). The process is usually described well by the autocatalytic model of Kamal [113]:

$$\frac{d\alpha}{dt} = k_1(T)(1-\alpha)^n + k_2(T)(1-\alpha)^n\alpha^m \tag{4.6}$$

where $k_1(T)$ and $k_2(T)$ represent the rate constants for the regular and autocatalyzed reactions, and n and m are the orders of reaction and autocatalysis. Taking the isoconversional derivative of eq. 4.6 gives the theoretical dependence for the isoconversional activation energy [21]:

$$E_\alpha \equiv E(\alpha, T) = \frac{A_1\exp(-E_1/RT)E_1 + \alpha^m A_2\exp(-E_2/RT)E_2}{A_1\exp(-E_1/RT) + \alpha^m A_2\exp(-E_2/RT)} \tag{4.7}$$

There are two problems with fitting eq. 4.7 to the experimental dependence of E_α on T and α. First, eq. 4.7 does not contain the parameter n, which has to be determined separately. Second, the parameters A_1 and A_2 enter the numerator and denominator as linear multipliers that makes it impossible to estimate reliably both parameters from fitting eq. 4.7. Note that using some numerical minimization procedure for fitting eq. 4.7 may converge at some values of A_1 and A_2. This does not mean that these are the true values that represent the global minimum. It is seen from eq. 4.7 that multiplying the resulting values by the same factor (e.g., 10) would not change the value of E_α. Therefore, the fitting procedure may converge at practically any values of A_1 and A_2 as long as their ratio remains the same. A solution to this problem is to rearrange eq. 4.7 to the following form [114]:

$$E_\alpha \equiv E(\alpha, T) = \frac{\gamma \exp(-E_1/RT)E_1 + \alpha^m \exp(-E_2/RT)E_2}{\gamma \exp(-E_1/RT) + \alpha^m \exp(-E_2/RT)} \tag{4.8}$$

where $\gamma = A_1/A_2$. Fitting the experimental Eα data to eq. 4.8 yields the values of γ, m, E_1 and E_2. An example of such fitting is presented in Figure 12 for crosslinking polymerization of bis(4-cyanatophenyl) sulfide [115].

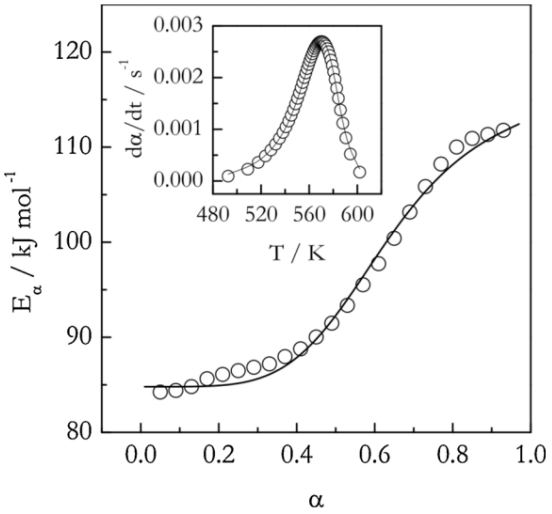

Fig. 12. Fitting isoconversional values of E_α (circles) for crosslinking polymerization of bis(4-cyanatophenyl) sulfide to eq. 4.8 (solid line) that yields the parameters E_1, E_2, γ, and m. Inset shows the results of fitting of the rate data (circles) to eq. 4.6 (solid line) to determine the parameters A_1, A_2, and n. Adapted from Galukhin et al. [115]. Copyright 2019 Wiley-VCH.

If the purpose of kinetic analysis is only to identify the activation energies of the regular and autocatalytic steps, fitting of eq. 4.8 is sufficient. If all parameters of the model (4.6) are needed, they can be determined from fitting the rate data, i.e., dα/dt. In this circumstance, the parameters determined from fitting eq. 4.8 can be plugged into eq. 4.6. In principle, this can reduce the number of the fit parameters in eq. 4.6 from 6 (E_1, E_2, A_1, A_2, n, m) to 2 (A_1 and n) that simplifies significantly the procedure of numerical minimization. However, this approach may be too restrictive to accomplish an accurate fit of the rate data. Then the accuracy of the fit can be improved by increasing the number of the fit parameters to 3 (A_1, A_2, n) or 4 (A_1, A_2, n, m). At any rate, it is recommended to use the E_1 and E_2 values obtained from fitting eq. 4.8 and keep them invariable while fitting eq. 4.6. This approach eliminates a major problem during numerical minimization. Because of the mutual correlation of the A and E values, their simultaneous variation can result in convergence at a local rather than the global minimum that renders the resulting values incorrect. Figure 12 shows an example of fitting eq. 4.6 to the rate data [115] to determine the parameters A_1, A_2, n, m.

The Kamal model holds when the crosslinking process occurs in the kinetic regime. Oftentimes, crosslinking polymerization changes from kinetic to diffusion regime at later stages of the process. This situation is detected as a change in E_α to either unusually small (< ~40 kJ mol^{-1}) or large (> ~100 kJ mol^{-1}) values at higher values of α. This transition is commonly associated with vitrification that can be detected by the techniques of rheometry [116] or temperature modulated DSC [116,117,118,119]. The transition or the mixed regime is described by a combination of the Rabinowitch [120] and Stolin et al. [121] models that yields [21] the effective rate constant for the process:

$$k_{ef}(T) = \frac{k(T)k_D(\alpha, T)}{k(T) + k_D(\alpha, T)} \tag{4.9}$$

Substitution of k_{ef} into eq. 1.1 followed by taking the isoconversional derivative leads to the isoconversional activation energy [21]:

$$E_\alpha \equiv E(\alpha, T) = \frac{E_D k(T) + E k_D(\alpha, T)}{k(T) + k_D(\alpha, T)} \tag{4.10}$$

where the subscript D denotes the parameters of the diffusion step. The diffusion rate constant in eq. 4.9 takes the following form [21]:

$$k_D(\alpha, T) = D_0 \exp\left(\frac{-E_D}{RT} + B\alpha\right) \tag{4.11}$$

where D_0 is the preexponential factor and B is the constant that accounts for changing the conditions of diffusion due to the progress of crosslinking.

With account of eq. 4.11, eq. 4.10 transforms into eq. 4.12

$$E_\alpha \equiv E(\alpha, T) = \frac{\gamma \exp(-E/RT)E_D + \exp(-E_D/RT + K\alpha)E}{\gamma \exp(-E/RT) + \exp(-E_D/RT + K\alpha)} \tag{4.12}$$

where $\gamma = A/D_0$. Fitting eq. 4.12 to experimental values of E_α yields E, E_D, B, and the ratio of the A and D_0 values [114]. Just as the A_1 and A_2 values in eq. 4.7, the A and D_0 values cannot be determined separately from fitting eq. 4.12. If needed, these values can be determined individually from fitting the rate data. This can be accomplished by using eq. 1.1 with $k(T)=k_{ef}(T)$ and $f(\alpha)=\alpha^m(1-\alpha)^n$. For accurate determination of the parameters of the diffusion step one should use the data related to the later stages of the process, i.e., the data that correspond to higher values of α. Subsequently, in the presence of the diffusion regime the parameters of the Kamal model (i.e., of the kinetic regime) are best determined from the earlier stages of the process (lower values of α).

Insights into selecting the respective intervals of α are offered elsewhere [122]. If the data do not reveal the occurrence of the diffusion regime, the Kamal model is applied to the whole range of α.

Note that the aforementioned approach to the treatment of the crosslinking kinetics can be implemented in other variants. For example, the diffusion rate constant (eq. 4.11) can be used [22] in the form of the Williams-Landel-Ferry equation:

$$k_D(\alpha, T) = D_0 \exp\left(\frac{C_1(T - T_g(\alpha))}{C_2 + T - T_g(\alpha)}\right) \tag{4.13}$$

where $T_g(\alpha)$ is the glass transition temperature as function of the reaction progress, and C_1 and C_2 are parameters whose typical values are about 40 and 50K correspondently. Also, the effect of diffusion can be introduced via the diffusion factor, $DF(\alpha,T)$ as follows:

$$\frac{d\alpha}{dt} = \left(\frac{d\alpha}{dt}\right)_{kin} DF(\alpha, T) \tag{4.14}$$

where $(d\alpha\, dt)kin$ is the kinetically controlled rate, which can be expressed by the Kamal model

(eq. 4.6). The diffusion factor can be presented by different equations that can be identified via measurements by regular and temperature modulated DSC [117,118,119,123]. It should also be noted that although the Kamal model is used most commonly, one can alternatively derive more specific models for describing the kinetics of crosslinking polymerization [124].

5. Deconvolution analysis

5.1 Basics

As explained in introduction, multi-step kinetics commonly manifest themselves in the form of overlapped rate peaks as measured by DSC or DTG. In the present context "deconvolution" means resolution of the overlapped rate peaks into individual rate peaks that can be expected to represent individual reaction steps. This can be accomplished by two approaches: mathematical deconvolution analysis (MDA) and kinetic deconvolution analysis (KDA). These approaches are explained below.

5.2 Mathematical deconvolution analysis

Reactions studied by thermal analysis are in many cases heterogeneous processes defined by the reaction geometry and kinetics of nucleation and interfacial reaction [125,126,127,128]. Similar issues may apply to the reactions in viscous liquid [129,130]. It is generally difficult to formulate rigorous kinetic equations for multi-step reactions whose steps defined by interplay of physical and geometrical factors because of the heterogeneous distributions of the reactive sites and the reaction interfaces in each reaction step [128]. One possible approach to such multi-step reactions is to set a kinetic relation between the individual reaction steps through the kinetic analysis based on the overall rate equation that considers the contributions, c_i, and kinetic models, $f_i(\alpha_i)$, [66,131] as a series of independent reaction steps (see section 2). The respective rate is as follows:

$$\frac{\mathrm{d}\alpha}{\mathrm{d}t} = \sum_{i=1}^{N} c_i A_i \exp\left(-\frac{E_i}{RT}\right) f_i(\alpha_i) \tag{5.1}$$

Mathematically, the contributions ci have the same meaning as the weights w_i used in sections 2 and 3. In eq. 5.1, $f_i(\alpha_i)$ represents physico-geometrical reaction mechanism of an individual reaction step. However, $f_i(\alpha_i)$ should be interpreted as an empirical function that describes the overall rate behavior for the reactions with the significant mutual dependence between the individual reaction steps. Thus, an empirical $f_i(\alpha_i)$ model which has large flexibility to fit different types of physico-geometrical rate behavior is preferable for analytical purposes. One such empirical model is that by Šesták and Berggren, SB(m, n, p) [132].

$$f(\alpha) = \alpha^m (1-\alpha)^n [-\ln(1-\alpha)]^p \tag{5.2}$$

Alternatively, a truncated Šesták–Berggren model with the first two terms multiplied by the model specific parameter q, i.e., $f(\alpha) = q\alpha^m(1-\alpha)^n$, is equally applicable [133,134,135]. In kinetic analysis based on eq. 5.1 the kinetic parameters of all reaction steps should be determined simultaneously through multiple nonlinear least squares analysis using an optimization algorithm. This procedure can be called kinetic deconvolution analysis (KDA). However, the reliability of the kinetic parameters determined by the nonlinear least squares analysis can be problematic because of the possible occurrence of local minima encountered during optimization. In addition, the estimated kinetic parameters can exhibit mutual correlation, e.g., a linear correlation between E and ln A values, also known as the kinetic compensation effect [136,137,138,139,140,141]. The occurrence of such effect can be expected for the parameters of the individual steps of the overlapped multi-step process. Thus, nearly perfect fits of the overall rate (Eq. 5.1) may be achieved by multiple combinations of different sets of the kinetic parameters for the individual steps. A practical method of avoiding this unwanted situation and, thus, for evaluating the kinetic parameters that possess physico-

chemical significance is to have reliable initial values for the process of numerical optimization. An alternative approach to separating overlapped rate peaks can be called mathematical deconvolution analysis (MDA). Its idea is to fit an overlapped peak by means of several mathematical functions $F(t)$ that have peak shapes. Then the overall rate can be expressed by the sum of the mathematical peak functions [131,142,143,144,145,146]:

$$\frac{\mathrm{d}\alpha}{\mathrm{d}t} = \sum_{i=1}^{N} F_i(t) \tag{5.3}$$

where $F_i(t)$ is the mathematical peak function, and N is the total number of peaks. Ideally, each peak should represent an individual reaction step. This procedure is usually applied to the overall rate peaks recorded under nonisothermal conditions. Application of MDA to isothermal data is also possible as long as the overall rate peaks show the signs of overlapping. Because the rate peaks of single-step reactions generally exhibit asymmetric shapes, the mathematical functions employed should also have asymmetric peak shapes [131,143,144,145,146,147]. For example, the Weibull and Frazer–Suzuki functions, which are shown in eqs. 5.4 and 5.5, respectively, have been successfully used for the MDA.

$$F(t) = a_0\left(\frac{a_3-1}{a_3}\right)^{\frac{1-a_3}{a_3}}\left(\frac{x-a_1}{a_2}+\left(\frac{a_3-1}{a_3}\right)^{\frac{1}{a_3}}\right)^{a_3-1}\exp\left[-\left(\frac{x-a_1}{a_2}+\left(\frac{a_3-1}{a_3}\right)^{\frac{1}{a_3}}\right)^{a_3}+\frac{a_3-1}{a_3}\right] \tag{5.4}$$

$$F(t) = a_0\exp\left[-\ln 2\left[\frac{\ln\left(1+2a_3\frac{x-a_1}{a_2}\right)}{a_3}\right]^2\right] \tag{5.5}$$

where a_0 is the amplitude, a_1 is the center, a_2 is the width, and a_3 is the shape parameters. Note that the choice of these mathematical functions is based on the shape analysis of the single-step reactions and assumes that the overlapped reaction steps are mutually independent. Because the individual steps may follow different $f_i(\alpha_i)$ models that give rise different kinds of the peak asymmetry, the choice of the mathematical functions for the individual steps should be made with care. Appropriate $F(t)$-functions should be selected for each reaction step with reference to the supplementary information about the process as well as the results of the subsequent kinetic analysis for the separated peaks. Although the selection of the functions is heuristic, it determines the kinetic relevance of MDA because eq. 5.3 is not a rate equation, but a mathematical approximation that describes the shape of the overall rate peak [128,131,145]. It is particularly difficult to carry out MDA successfully when the contributions of the individual reaction steps to the overall rate have the opposite signs.

Figure 13 shows an example of MDA followed by kinetic analysis of the separated peaks for the thermal dehydrochlorination of polyvinyl chloride (PVC) that consist of two overlapping process [66,145]. When a multistep process is adequately separated by MDA with significant relevance to the actual reaction mechanism, the *ci* values are calculated as the ratio of the areas of an individual and overall peaks (Figure 13(a)). If the *ci* values are known a priori or expected from the reaction mechanism, the estimated c_i values can serve as a guide to assess the adequateness of MDA. Depending on the nature of the overlapped process, the c_i values may change when changing the measurement conditions, e.g., the heating rate or a temperature program in general. If the estimated c_i values are practically invariant for a series of the overall rate peaks measured under different conditions, MDA is likely to yield a series of individual rate peaks that respectively represent individual reaction steps. Then, each separated rate peak

is analyzed under the assumption of the single-step kinetics by using the techniques overviewed in the previous recommendations of the ICTAC kinetics committee [1]. First, for each separated i-th peak an isoconversional method should be applied to evaluate $E_{\alpha,i}$ values at different α_i. If a separated peak really represents an individual reaction step, the resulting $E_{\alpha,i}$ values should be practically independent of α_i. Finding that $E_{\alpha,i}$ is nearly constant for all separated peaks, supports both adequateness of MDA and validity of the single-step assumption for all individual reactions. After that a variety of techniques [1] such as master plot analysis can be used to determine $f_i(\alpha_i)$ and A_i [148,149]. Figure 13(b) clearly shows that the isoconversional values of E_α determined for the overall process varies strongly with α, as expected for a multi-step process. Nevertheless, the $E_{\alpha,\mathrm{i}}$ values obtained for the separated reactions remain practically constant in the respective α_i ranges. Moreover, $E_{\alpha,i}$ values for the first and second processes are coincident with the E_α values obtained for the overall reaction for the small and large overall α values, respectively. The dehydrochlorination process could be fitted by a nucleation and growth kinetic model (indicating that the decomposition starts in reactive sites of the PVC molecule) followed by a diffusion controlled kinetic model, which was supported by the results of microscopic observations [66]. The kinetic curves simulated by using the resulting kinetic parameters reproduce not only the linear heating experiments used for the analysis but also experimental curves obtained under other conditions, such as isothermal heating (Figure 13(c)). This validates the results of the kinetic analysis and accomplishes one of the major objectives of kinetic analysis that is the ability of making predictions of the reaction kinetics. In more complex cases, MDA may result in variations of c_i and $E_{\alpha,i}$ values depending on reaction conditions and α_i, respectively. The variations may be caused by problematic MDA (e.g., inappropriate selection of the mathematical peak functions) or by the complex nature of the separated reaction steps. Even if a constant $E_{\alpha,i}$ value was found for a reaction step, the master plot analysis would not necessarily yield $f_i(\alpha_i)$ that represents the actual physico-geometrical mechanism of the reaction step, i.e., the mechanism that forms the foundation of the corresponding $f(\alpha)$ model. This is because MDA disregards any mutual dependence between the individual reaction steps. When the individual reaction steps are really independent of each other, it is possible to use the estimated $f_i(\alpha_i)$ functions for physico-geometrical interpretation. However, for a multi-step process with the mutually dependent reaction steps the $f_i(\alpha_i)$ functions estimated for the separated rate peaks should be treated as empirical functions representing the overall kinetic behavior.

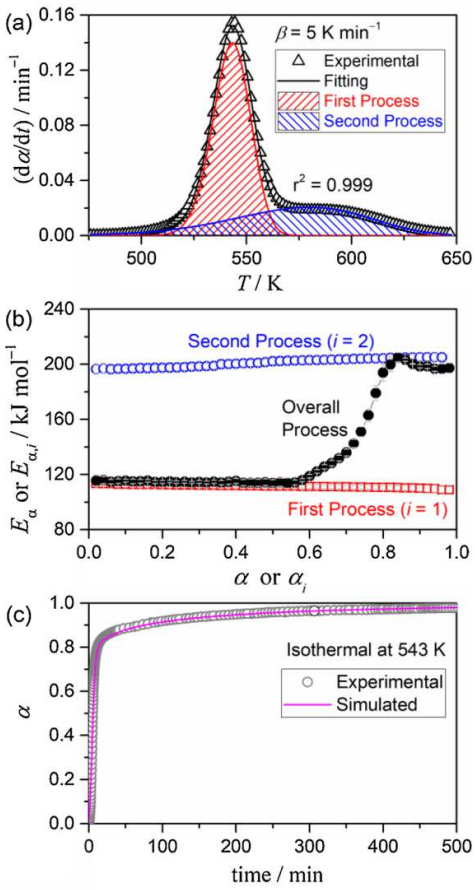

Fig. 13. Mathematical deconvolution analysis (MDA) and subsequent isoconversional analysis for the thermal dehydrochlorination of polyvinyl chloride (PVC): (a) a typical result of MDA (β = 5 K min^{-1}) performed using the Frazer–Suzuki function, (b) $E\alpha$ values as a function of the reaction fraction, as determined by Friedman method, for the overall process and for the separated first and second processes, and (c) an isothermal experimental curve at 543 K and a curve simulated using the kinetic parameters resulted of the kinetic analysis. Adopted from Perejon et al. [145] (DOI: https://doi.org/10.1021/jp110895z), with permission. Copyright 2011 American Chemical Society.

5.3 Kinetic deconvolution analysis

Successful kinetic analysis based on MDA is not always possible because the mathematical peak functions may not be adequate for separation of the individual reaction steps. In this situation, the results of kinetics analysis of the individual steps can provide kinetic parameters to be used as the initial values for more careful KDA based on eq. 5.1. More reliable initial values for KDA are obtained when MDA results in adequate separation. Optimization of the kinetic parameters through KDA reformulates the kinetic description based on eq. 5.1. The kinetic parameters determined by KDA may be practically the same as those estimated by MDA if the results of the latter are accurate. Otherwise, KDA can improve a problematic kinetic description obtained in preliminary analysis. Considering that KDA makes use of $f_i(\alpha_i)$ in the form of the empirical SB(m,n,p) model (eq. 5.2) to separate the overall rate peak into the rate peaks for the individual steps, the latter can be analyzed further by the techniques developed for single-step kinetics [1]. In particular, one can apply the master plots method to see if the kinetics for the individual steps follow the $f(\alpha)$ models that have a physico-geometrical meaning. If this is the case, the analysis can provide some mechanistic insights. KDA is applicable to kinetic data recorded under any temperature programs [150,151,152,153] as shown in Figure 14 for the two-step thermal decomposition of $Mg(OH)_2$ under linear nonisothermal, isothermal, and constant transformation rate conditions [152]. When the

contributions and kinetic parameters of each reaction step are invariant with respect to different temperature programs, the kinetic curves measured under different conditions can be simultaneously subjected to KDA. On the other hand, possible changes in the kinetic parameters obtained under different reaction conditions can be identified by applying KDA to the respective curves separately. When the chemical reaction in each reaction step and a relationship between the steps has been revealed by the supplementary techniques, the individual reactions making opposing contributions (i.e, mass loss versus mass gain or exothermic versus endothermic) to the overall rate process can also be analyzed by KDA. This has been recently demonstrated for the thermal decomposition and subsequent oxidation or carbonation processes [153,154,155]. In some cases of partially overlapping reactions, the overall kinetic data measured by different techniques (e.g., TGA and DSC) may give rise to respectively different kinetic curves even though the measurements are made simultaneously. In such cases different techniques can exhibit different relationships between, say, two individual steps. For example, both steps are characterized by mass-losses but one being exothermic and another endothermic. Under such circumstances, the overall rate curves measured by different techniques are represented by different rate equations [156,157]. When the reaction kinetics of such multi-step process is tracked by using simultaneous TGA–DSC, the *ci* values for the respective kinetic equations are calculated using the initial and final part of the kinetic data.

$$\frac{c_1(\mathrm{DSC})}{c_1(\mathrm{DTG})} = \left[\left(\frac{\mathrm{d}\alpha}{\mathrm{d}t}\right)_{\mathrm{DSC}} / \left(\frac{\mathrm{d}\alpha}{\mathrm{d}t}\right)_{\mathrm{DTG}}\right]_{\mathrm{initial}} \quad \text{and} \quad \frac{c_2(\mathrm{DSC})}{c_2(\mathrm{DTG})} = \left[\left(\frac{\mathrm{d}\alpha}{\mathrm{d}t}\right)_{\mathrm{DSC}} / \left(\frac{\mathrm{d}\alpha}{\mathrm{d}t}\right)_{\mathrm{DTG}}\right]_{\mathrm{final}} \tag{5.6}$$

Then, the kinetic curves for each reaction step are obtained as follows without any preliminary kinetic analyses and assumptions [156,157].

$$\frac{\mathrm{d}\alpha_1}{\mathrm{d}t} = \frac{c_2(\mathrm{DTG})}{c_1(\mathrm{DSC}) - c_1(\mathrm{DTG})}\left[\left(\frac{\mathrm{d}\alpha}{\mathrm{d}t}\right)_{\mathrm{DSC}} - \frac{c_2(\mathrm{DSC})}{c_2(\mathrm{DTG})}\left(\frac{\mathrm{d}\alpha}{\mathrm{d}t}\right)_{\mathrm{DTG}}\right] \tag{5.7}$$

$$\frac{\mathrm{d}\alpha_2}{\mathrm{d}t} = \frac{c_1(\mathrm{DTG})}{c_1(\mathrm{DTG}) - c_1(\mathrm{DSC})}\left[\left(\frac{\mathrm{d}\alpha}{\mathrm{d}t}\right)_{\mathrm{DSC}} - \frac{c_1(\mathrm{DSC})}{c_1(\mathrm{DTG})}\left(\frac{\mathrm{d}\alpha}{\mathrm{d}t}\right)_{\mathrm{DTG}}\right] \tag{5.8}$$

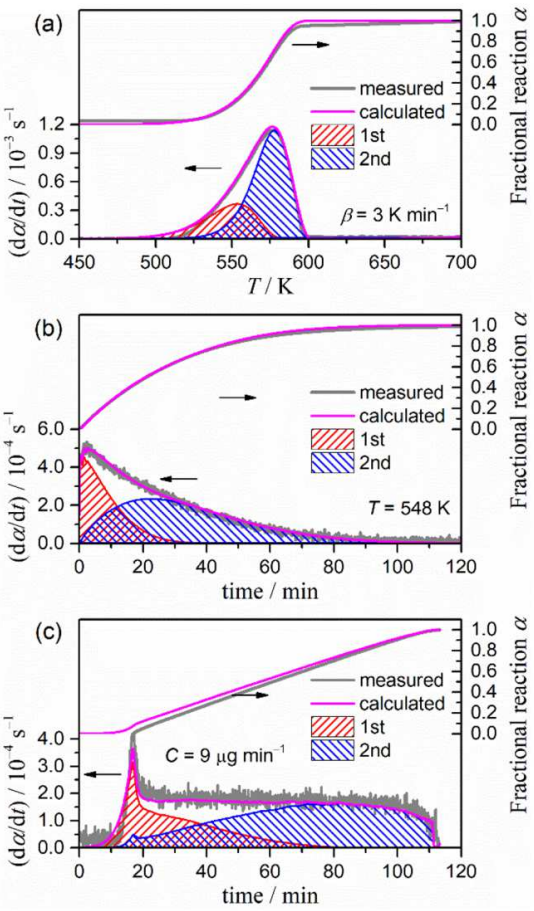

Fig. 14. Typical results of KDA for the thermal decomposition of $Mg(OH)_2$ under various heating conditions: (a) linear nonisothermal, (b) isothermal, and (c) constant transformation rate modes. (Adopted from Iwasaki et al. [152] (DOI: https://doi.org/10.1021/acs.jpcc.9b09656), with permission. Copyright 2020 American Chemical Society.

Thus, MDA as a preliminary kinetic approach can be skipped. Followed by the kinetic analysis of the separated rate peaks, the kinetic features of the individual steps can be revealed separately by KDA for the mass and enthalpy changes as shown in Figure 15 for the thermolysis of ammonium dinitramide [156].

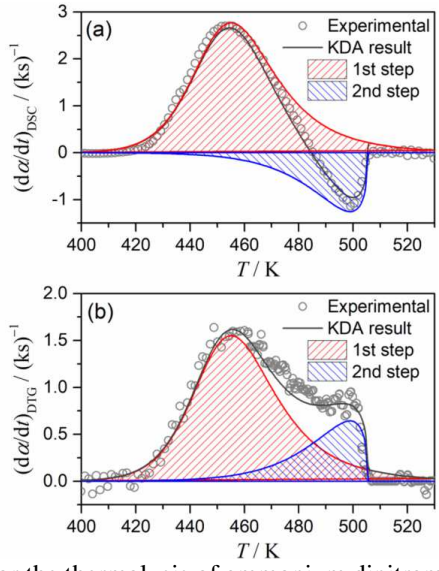

Fig. 15. Typical results of KDA for the thermolysis of ammonium dinitramide comprising two-step mass-loss process accompanied by exothermic and endothermic effects (β = 5 K min^{-1}): (a) kinetic data from DSC and (b)

KDA is a simple kinetic evaluation based on eq. 5.1. It can be applied to many different types of partially overlapped multi-step processes, just as MDA can. Yet, the physico-chemical and physico-geometrical significance of the kinetic results depends on the type of a multi-step process. For a multi-step process composed of independent reaction steps one can expect an exact kinetic solution. However, when the individual reactions become mutually dependent such as for consecutive or competing reactions, the results of KDA or MDA become semi-empirical and provide only an approximate formal solution. Even though, the results can still be used for simulating the overall reaction under reaction conditions comparable to those used in kinetic analyses. The kinetic results can be analyzed further for revealing the physico-chemical and physico-geometrical features of complex heterogeneous processes, when enough supplementary experimental evidence is available. A successful example of such analysis is seen for the isothermal process that involves consecutive surface (SR) and phase-boundary controlled reaction (PBR) as originally formulated by Mampel [158]. Recently, the kinetic model has been reconstructed by Favergeon et al. [159,160] as nucleation and anisotropic growth model, and the differential kinetic equations for this type of consecutive reactions have been derived by Ogasawara and Koga [161] to allow for simplifying kinetic evaluations. For example, the consecutive first-order SR and three dimensional PBR model at a constant temperature is described by [161]:

$$\text{a)}\ t \le 1/k_{\mathrm{PBR}(3)}\text{:}$$

$$\frac{\mathrm{d}\alpha}{\mathrm{d}t} = -3k_{\mathrm{PBR}(3)}\left[\left(1 + 2\frac{k_{\mathrm{PBR}(3)}}{k_{\mathrm{SR}}} + 2\left(\frac{k_{\mathrm{PBR}(3)}}{k_{\mathrm{SR}}}\right)^2\right)\exp(-k_{\mathrm{SR}}t) - (k_{\mathrm{PBR}(3)}t)^2 + 2k_{\mathrm{PBR}(3)}\left(\frac{k_{\mathrm{PBR}(3)}}{k_{\mathrm{SR}}} + 1\right)t - \left(1 + 2\frac{k_{\mathrm{PBR}(3)}}{k_{\mathrm{SR}}} + 2\left(\frac{k_{\mathrm{PBR}(3)}}{k_{\mathrm{SR}}}\right)^2\right)\right]$$

$$\text{b)}\ t \ge 1/k_{\mathrm{PBR}(3)}\text{:}$$

$$\frac{\mathrm{d}\alpha}{\mathrm{d}t} = 3k_{\mathrm{PBR}(3)}\exp(-k_{\mathrm{SR}}t)\left[2\left(\frac{k_{\mathrm{PBR}(3)}}{k_{\mathrm{SR}}}\right)^2\left(\exp\left(\frac{k_{\mathrm{SR}}}{k_{\mathrm{PBR}(3)}}\right) - 1\right) - \left(1 + 2\frac{k_{\mathrm{PBR}(3)}}{k_{\mathrm{SR}}}\right)\right] \tag{5.9}$$

where k_{SR} and $k_{\mathrm{PBR}(n)}$ are the rate constants for SR and PBR, respectively. After optimizing the k_{SR} and $k_{\mathrm{PBR}(n)}$ values for each isothermal kinetic curve at different temperatures, the kinetic parameters of SR and PBR are determined individually from the temperature dependence of the respective rate constants [152,161,162,163]. A universal kinetic description of SR and PBR process over a range of different temperatures and partial pressures of evolved gas is a current accomplishment of the kinetic approach [164,165]. However, kinetic modeling for more complex consecutive or competing reactions in the heterogeneous systems is a crucial future task.

5.4 Additional remarks on the deconvolution analysis

(1) Kinetic analysis of overlapping multi-step reactions is quite challenging because of the reaction diversity, i.e., a multitude of situations, in which various physico-chemical and physico-geometrical features of the sample and reaction can contribute the kinetic complexity in addition to independent, consecutive, or competitive reaction steps.

(2) Detailed characterization of the sample from compositional, morphological, crystallographic, and spectroscopic standpoints is necessary for adequate understanding of multi-step reactions, because sometimes the sample properties are a direct cause of the multi-step kinetic behavior as seen for composite materials and samples with broad particle size distribution [166].
(3) Measurements under a wide variety of temperature programs (nonisothermal, isothermal, rate controlled) and atmospheric conditions are required for understanding the origins of the multi-step reaction behavior. Simultaneous measurements that combine different thermal analysis methods or other techniques can be the key for successful kinetic evaluations via MDA and KDA. Combining the experimental kinetic data obtained from different measurements always provides valuable information for elucidating the kinetics of multi-step reactions [156,167] While relevant to any multi-step kinetic analysis, these remarks are especially important when MDA and KDA are used as an empirical kinetic procedure.

6. Conclusions.

The present recommendations have discussed four different approaches that can be used to tackle multi-step kinetics efficiently. Computationally, none of these approaches is as simple as the approaches used for analysis of single-step kinetics. The latter can commonly be reduced to linear regression that normally is not associated with computational difficulties. The multi-step kinetics are analyzed by nonlinear regression that requires the use of numerical methods of multiparameter optimization. There are many software packages that perform such optimization to fit multi-parameter models to experimental data. They can be used to implement any of the approaches discussed in this paper. However, one should always judge the obtained kinetic parameters critically. There are no algorithms of numerical optimization that always produce a correct solution for any type of a model and the data of any quality. The necessary condition of a correct solution is its uniqueness. It should be verified by making sure that the final optimized values of the kinetic parameters remain the same when using significantly different initial values as a starting point of optimization. This secures that optimization converges to the global rather than a local minimum. Closely related is the issue of the number of kinetics parameters that need to be optimized. The smaller this number the better are the chances for optimization to find the global minimum and, thus, to yield a unique solution. Thus, one should be advised to aim at constructing kinetic models with fewer reaction steps. The need to introduce additional reaction steps into a model should be justified by physical rather than purely statistical reasons. The optimization procedures do rely on statistical parameters to accomplish the best goodness of fit. Nevertheless, the numerical values of these parameters (e.g., RSS or r^2) cannot be used as the metrics for evaluating the meaningfulness of a kinetic model and its parameters. Although a meaningful model must necessarily fit the data, a model that fits is not necessarily meaningful. Note that perfect fits can be accomplished by spline interpolation that has no kinetic meaning whatsoever. The fact that a multi-step model provides a statistically adequate description of a process does not mean that this model is unique. It is not unusual when one finds another multi-step model that describes the same process equally well. In the statistical sense, equally well means that, for example, the RSS values for two models do not differ significantly based on the F-test. In this situation, distinguishing between the models may be problematic. If the models are represented by mathematical functions that differ significantly (e.g., exponential and power law), the models may likely be distinguished by comparing the accuracy of predictions made outside the range of experimental conditions used for establishing these models. Alternatively, one may distinguish between the models by utilizing additional analytical techniques capable of furnishing mechanistic insights. Yet, it should be kept in mind that alternative models are not always mutually exclusive.

For instance, the situation may arise when the crystallization kinetics of a polymer is equally well described by the Turnbull-Fisher and Hoffman-Lauritzen models. These models are not mutually exclusive as they both are physically meaningful representations of crystallization kinetics.

Last but not least, it must be recognized that if the purpose of multi-step kinetic analysis is obtaining insights into a process, the necessary attribute of a model is meaningfulness. To put it simply, the model must make sense in the context of a process being analyzed. Otherwise, neither model nor its parameters can lend themselves to a physically meaningful interpretation. The interpretability is accomplished via experimental evidence and theoretical understanding that can link a model to the process in question. On the other hand, kinetic analysis can pursue purely technical goals such as making kinetic predictions. In this case, the sufficient attribute of a model is numerical robustness that is easier accomplished in models with fewer parameters.

Acknowledgements.

The authors thank all their colleagues who actively participated in the discussions of the present project during the 16th ICTAC Congress. Special thanks are due to those who read the draft document and provided written comments: Dimitris Achilias, Dimitrios Bikiaris, Petru Budrugeac, Konstantinos Chrissafis, Jordi Farjas, Rafael Font, Jiri Malek, Jose Maria Morancho, George Papageorgiou, Crisan Popescu, Xavier Ramis, Pere Roura, and Peter Simon.

Declaration of interests

The authors declare that they have no known competing financial interests or personal relationships that could have appeared to influence the work reported in this paper.

References

[1] S. Vyazovkin, A. K. Burnham, J. M. Criado, L. A. Pérez-Maqueda, C. Popescu, N. Sbirrazzuoli, ICTAC Kinetics Committee recommendations for performing kinetic computations on thermal analysis data, Thermochim. Acta 520 (2011) 1-19.

[2] S. Vyazovkin, K. Chrissafis, M. L. Di Lorenzo, N. Koga, M. Pijolat, B. Roduit, N. Sbirrazzuoli, J. J. Suñol, ICTAC Kinetics Committee recommendations for collecting experimental thermal analysis data for kinetic computations, Thermochim. Acta 590 (2014) 1-23.

[3] S. Vyazovkin, Isoconversional kinetics of polymers: The decade past, Macromol. Rapid Commun. 38 (2017) 1600615

[4] D. Jelić, T. Liavitskaya, E. Paulechka, S. Vyazovkin, Accelerating effect of poly(vinylpyrrolidone) matrix on thermal decomposition of malonic acid, Ind. & Eng. Chem. Res. 58 (2019) 2891–2898.

[5] V. L. Stanford, T. Liavitskaya, S. Vyazovkin, Effect of inert gas pressure on reversible solidstate decomposition, J. Phys. Chem. C 123 (2019) 21059-21065.

[6] G. T. Long, S. Vyazovkin, N. Gamble, C. A. Wight, Hard to swallow dry: Kinetics and mechanism of the anhydrous thermal decomposition of acetylsalicylic acid, J. Pharm. Sci. 91 (2002) 800-809.

[7] S. Vyazovkin, N. Sbirrazzuoli, Kinetic methods to study isothermal and nonisothermal epoxy-anhydride cure, Macromol. Chem. Phys. 200 (1999) 2294-2303.

[8] H. E. Kissinger, Variation of peak temperature with heating rate in differential thermal analysis, J. Res. Natl. Bur. Stand. 57 (1956) 217-221.

[9] H. E. Kissinger, Reaction kinetics in differential thermal analysis, Anal. Chem. 29 (1957) 1702-1706.

[10] S. Vyazovkin, L. Vincent, N. Sbirrazzuoli, Thermal denaturation of collagen analyzed by isoconversional method, Macromol. Biosci. 7 (2007) 1181-1186.

[11] S. Vyazovkin, B. Yancey, K. Walker, Polymer melting kinetics appears to be driven by heterogeneous nucleation, Macromol. Chem. Phys. 215 (2014) 205-209.

[12] R. Farasat, S. Vyazovkin, Nanoconfined solid-solid Transitions: Attempt to separate the size and surface effects, J. Phys. Chem. C, 119 (2015) 9627–9636.

[13] J. Farjas, N. Butchosa, P. Roura, A simple kinetic method for the determination of the reaction model from non-isothermal experiments, J. Therm. Anal. Calorim. 102 (2010) 615–625.
[14] E.Moukhina, Determination of kinetic mechanisms for reactions measured with thermoanalytical instruments, J. Therm. Anal. Calorim. 109 (2012) 1203-1214.
[15] J. Opfermann, Kinetic analysis using multivariate non-linear regression I. Basic concepts. J. Therm. Anal. Calorim. 60 (2000) 641-658.
[16] E. Moukhina, Thermal decomposition of AIBN Part C: SADT calculation of AIBN based on DSC experiments, Thermochim. Acta 621 (2015) 24-35.
[17] M. Malow, K.-D. Wehrstedt, M. Manolov, Thermal decomposition of AIBN Part A: Decomposition in real scale packages and SADT determination, Thermochim. Acta 621 (2015) 1-5.
[18] M. J. G. Fait, E. Moukhina, M. Feist, Hans-Joachim Lunk, Thermal decomposition of ammonium paratungstate tetrahydrate: New insights by a combined thermal and kinetic analysis, Thermochim Acta 637 (2016) 38-50.
[19] E. Moukhina, Initial kinetic parameters for the model-based kinetic method, High Temperatures-High Pressures, 42 (4) (2013), 287-302.
[20] S. Sourour, M.R. Kamal, Differential Scanning Calorimetry of Epoxy Cure, Isothermal Cure Kinetics, Thermochem. Acta 14 (1976), 41-59.
[21] S. Vyazovkin, N. Sbirrazzuoli, Mechanism and kinetics of epoxy-amine cure studied by differential scanning calorimetry, Macromolecules, 29 (1996) 1867 - 1873.
[22] H. J. Flammersheim, J. Opfermann, Formal kinetic evaluation of reactions with partial diffusion control, Thermochim. Acta 337 (1999) 141-148.
[23] J.R. Opfermann, E. Kaisersberger, H.J. Flammersheim, Model-free analysis of thermoanalytical data-advantages and limitations, Thermochim. Acta 391 (2002) 119-127.
[24] ASTM E2070-13(2018) Standard Test Method for Kinetic Parameters by Differential Scanning Calorimetry Using Isothermal Methods, Annual Book of ASTM Standards, vol. 14.05, ASTM International,West Conshohocken, PA, 2019.
[25] S. Vyazovkin, Kinetic effects of pressure on decomposition of solids, Int. Rev. Phys. Chem., 39 (2020) 35-66.
[26] S. Vyazovkin, N. Sbirrazzuoli, Isoconversional Analysis of Nonisothermal Crystallization of a Polymer Melt, Macromol. Rapid Commun. 23 (2002) 766-770.
[27] E.Moukhina, Comparison of isothermal predictions based on model-free and model-based kinetic methods, J.Test.Eval. 42 (2014) 1377-1386.
[28] S. Vyazovkin, N. Sbirrazzuoli, Effect of viscosity on the kinetics of initial cure stages. Macromol. Chem. Phys. 201 (2000) 199-203.
[29] P. Hanbaba, Reaktionskinetische Untersuchungen zur kohlenwasserstoffentbindung aus steinkohlen bie niedrigen aufheizgeschwindigkeiten, Dissertation, University of Aachen (1967).
[30] D. B. Anthony, J. B. Howard, Coal devolatilization and degasification, AICHE J. 22 (1976) 625-656.
[31] A. K Burnham, M. S. Oh, R. W. Crawford, Pyrolysis of Argonne Premium Coals: activation energy distributions and related chemistry, Energy Fuels 3 (1989) 42-55.
[32] R. L. Braun, A. K. Burnham, J. G. Reynolds, J. E. Clarkson, Pyrolysis kinetics for lacustrine and marine source rocks by programmed micropyrolysis, Energy Fuels 5 (1991) 192-204.
[33] B. P. Boudreau, B. R. Ruddick, On a reactive continuum representation of organic matter diagenesis, Amer. J. Sci. 291 (1991) 507-538.
[34] J. Cai, New distributed activation energy model: numerical solution and application to pyrolysis kinetics of some types of biomass, Bioresource Tech. 99 (2008) 2795-2799.
[35] G. Várhegyi, B. Bobály, E. Jakab, H. Chen, Thermogravimetric study of biomass pyrolysis kinetics: a distributed activation energy model with prediction tests, Energy Fuels 25 (2011) 24-32.
[36] Z. Chen, M. Hu, X. Zhu, D. Guo, S. Liu, Z. Hu, B. Xiao, J. Wang, M. Laghari, Characteristics and kinetic study on pyrolysis of five lignocellulosic biomass via thermogravimetric analysis, Bioresource Tech. 192 (2015) 441-450.
[37] G. Várhegyi, L. Wang, Ø. Skreiberg, Towards a meaningful non-isothermal kinetics for biomass materials and other complex organic samples, J. Therm. Anal. Calor. 133 (2018) 703-712.

[38] J. Giuntoli, S. Arvelakis, H. Spliethoff, W. de Jong, A. H. M. Verkooijen, Quantitative and kinetic thermogravimetric Fourier transform infrared (TG-FTIR) study of pyrolysis of agricultural residues: influence of different pretreatments, Energy Fuels 23 (2009) 5695-5706.
[39] A. K. Burnham, Global kinetic analysis of complex materials, Energy Fuels 13 (1999) 1-22.
[40] A. Bhargava, P. van Hees, B. Andersson, Pyrolysis modeling of PVC and PMMA using a distributed reactivity model, Polymer Degrad. Stability 129 (2016) 199-211.
[41] W. Tang, C. Wang, D. Chen, Kinetic studies on the pyrolysis of chitin and chitosan, Polymer Degrad. Stability 87 (2005) 389-394.
[42] A. K. Burnham, An nth-order Gaussian energy distribution model for sintering, Chem. Eng. J. 108 (2005) 47-50.
[43] G. Carter, P. Bailey, D. G. Armour, The precise deduction of desorption activation distributions from thermal evolution spectra, Vacuum 34 (1984) 797-800.
[44] H. Wittkopf, Calculation of desorption energy distribution applied to temperature programmed H2O desorption from silicate glass surface, Vacuum 37 (1987) 819-823.
[45] Z. Du, A. F. Sarofim, J. P. Longwell, Activation energy distribution in temperature programmed desorption: modeling and application to the soot-oxygen system, Energy Fuels 4 (1990) 296-302.
[46] E.G. Seebauer, Quantitative extraction of continuous distributions of energy states and preexponential factors from thermal desorption spectra, Surface Science 316 (1994) 391-405.
[47] P. J. Barrie, Analysis of temperature-programmed desorption (TPD) data for characterization of catalysts containing a distribution of adsorption sites, Phys. Chem. Chem. Phys. 10 (2008) 1688-1696.
[48] P. Staszczuk, D. Sternik, V. V. Kutarov, Analysis of the energy heterogeneity of HgBa2Ca2Cu3O8+δ surfaces Q-TG and Q-DRG data, J. Therm. Anal. Calor. 69 (2002) 23-36.
[49] E. M. Suuberg, Approximate solution technique for nonisothermal, Gaussian distributed activation energy models, Comb. Flame 50 (1983) 243-245.
[50] A. K Burnham, Vitrimat2: a modified model of vitrinite maturation and reflectance, Lawrence Livermore National Laboratory Report UCRL-ID-109903, February 1992.
[51] P. Ungerer, R. Pelet, Extrapolation of the kinetics of oil and gas formation from laboratory experiments to sedimentary basins, Nature 327 (1987) 52-54.
[52] A. K. Burnham, R. L. Braun, H. R. Gregg, A. M. Samoun, Comparison of methods for measuring kerogen pyrolysis rates and fitting kinetic parameters, Energy Fuels 1 (1987) 452-458.
[53] E. A. Dorko, W. Bryant, T. L. Regulinski, Solid state reaction kinetics IV: the analysis of chemical reactions by means of the Weibull function, Anal. Calor. 3 (1974) 505-510.
[54] Lj. Kolar-Anić, S. Vellijković, S. Kapor, B. Dubljević, Weibull distribution and kinetics of heterogeneous processes, J. Chem. Phys. 63 (1975) 663-668.
[55] C. C. Lakshmanan, N, White, A new distributed activation energy model using Weibull distribution for the representation of complex kinetics, Energy Fuels 8 (1994) 1158-1167.
[56] Lj. Kolar-Anić, S. Vellijković, Statistical foundations of heterogeneous kinetics, J. Chem. Phys. 63 (1975) 669-673.
[57] P. J. Crickmore, Power law models of descriptors of the kinetics of complex systems: temperature effects, Can. J. Chem. Eng. 67 (1989) 392-396.
[58] B. Janković, Identification of the effective distribution function for determination of the distributed activation energy models using the maximum likelihood method: isothermal thermogravimetric data, Intl. J. Chem. Kin. 41 (2009) 27-44.
[59] J. Cai, C. Jin, S. Yang, Y. Chen, Logistic distributed activation energy model—Part 1: derivation and numerical parametric study, Bioresource Tech. 102 (2011) 1556-1561.
[60] A. K. Burnham, R. K. Weese, A. P. Wemhoff, J. L. Maienschein, A historical and current perspective on predicting cookoff behavior, J. Therm. Anal. Calor. 89 (2007) 407-415.
[61] J. Tarrío-Saavedra, J. López-Beceiro, S. Naya, M. Francisco-Fernández, R. Artiaga, Simulation study for generalized logistic function in thermal data modeling, J. Therm. Anal. Calor. 118 (2014) 1253-1268.
[62] A. K. Burnham, Use and misuse of logistic equations for modeling chemical kinetics, J. Therm. Anal. Calor. 127 (2017) 1107-1116.

[63] N. Sbirrazzuoli, D. Brunel. Computational neural networks for mapping calorimetric data: application of feed-forward neural networks to kinetic parameters determination and signal filtering. Neural Comput. & Applic. 5 (1997) 20-32.
[64] D. M. J. Purnomo, T. Richter, M. Bonner, R. Vaidyanathan, G. Rein, Role of optimisation method on kinetic inverse modelling of biomass pyrolysis at the microscale, Fuel 262 (2020) 116251.
[65] J. Hillier, T. Bezzant, T. H. Fletcher, Improved method for the determination of kinetic parameters from non-isothermal thermogravimetric analysis (TA) data, Energy Fuels 24 (2010) 2841-2847.
[66] P. E. Sánchez-Jiménez, A. Perejón, J. M. Criado, M. J. Diánez, L. A. Pérez-Maqueda, Kinetic model for thermal dechlorination of poly(vinyl chloride), Polymer 51 (2010) 3998-4007.
[67] F. Richter, G. Rein, Reduced chemical kinetics for microscale pyrolysis of softwood and hardwood, Bioresource Tech. 301 (2020) 122619.
[68] B. Roduit, M. Hartmann, P. Folly, A. Sarbach, R. Baltensperger, Prediction of thermal stability of materials by modified kinetic and model selection approaches based on limited amount of experimental points, Thermochim. Acta 579 (2014) 31-39.
[69] E. B. Huss, A. K. Burnham, Gas evolution during pyrolysis of various Colorado oil shales, Fuel 61 (1982) 1188-1196.
[70] S. Vyazovkin, In: The Handbook of Thermal Analysis & Calorimetry: Recent Advances, Techniques and Applications, Vol.6, 2nd Ed; Eds.: Vyazovkin, S.; Koga, N.; Schick, C. Elsevier: Amsterdam, 2018, p. 131.
[71] T. Ozawa, A new method of analyzing thermogravimetric data, Bull. Chem. Soc. Japan 38 (1965) 1881-1886.
[72] J. H. Flynn, L. A. Wall, A quick, direct method for the determination of activation energy from thermogravimetric data, J. Polym. Sci. C, Polym. Lett. 4 (1966) 323-328.
[73] J. H. Flynn, L. A. Wall, General treatment of the thermogravimetry of polymers, J. Res. Nat. Bur. Standards, Part A 70 (1966) 487-523.
[74] T. Akahira, T. Sunose, Method of determining activation deterioration constant of electrical insulating materials. Res. Report Chiba Inst. Technol. (Sci. Technol.) 16 (1971) 22-31.
[75] M. J. Starink, The determination of activation energy from linear heating rate experiments: a comparison of the accuracy of isoconversion methods. Thermochim. Acta 404 (2003) 163-176.
[76] S. Vyazovkin, Isoconversional Kinetics of Thermally Stimulated Processes; Springer: Heidelberg, 2015.
[77] S. Vyazovkin, Modification of the integral isoconversional method to account for variation in the activation energy. J. Comput. Chem. 22 (2001) 178-183.
[78] J. Farjas, P. Roura, Isoconversional analysis of solid state transformations. A critical review. Part II. Complex transformations, J. Therm. Anal. Calorim. 105 (2011) 767–773.
[79] S. Vyazovkin, D. Dollimore, Linear and nonlinear procedures in isoconversional computations of the activation energy of thermally induced reactions in solids. J. Chem. Inf. Comp. Sci. 36 (1996) 42-45.
[80] C. Popescu, Integral method to analyze the kinetics of heterogeneous reactions under nonisothermal conditions. A variant on the Ozawa-Flynn-Wall method. Thermochim. Acta 285 (1996) 309-323.
[81] S. Vyazovkin, Evaluation of the activation energy of thermally stimulated solid-state reactions under an arbitrary variation of the temperature. J. Comput. Chem. 18 (1997) 393-402.
[82] P. Simon, P. S. Thomas, J. Okuliar, A. S. Ray, An incremental integral isoconversional method. Determination of activation parameters. J. Therm. Anal. Calorim. 72 (2003) 867-874.
[83] W. Tang, D. Chen, An integral method to determine variation in activation energy with extent of conversion, Thermochim. Acta 433 (2005) 72-76.
[84] A. Ortega, A simple and precise linear integral method for isoconversional data. Thermochim. Acta, 474 (2008) 81-86.
[85] J. Cai, S. Chen, New iterative linear integral isoconversional method for the determination of the activation energy varying with the conversion degree. J. Comput. Chem. 30 (2009) 1986-1991.

[86] P. Budrugeac, An iterative model-free method to determine the activation energy of nonisothermal heterogeneous processes, Thermochim. Acta 511 (2010) 8-16.
[87] P. Budrugeac, An iterative model-free method to determine the activation energy of heterogeneous processes under arbitrary temperature programs, Thermochim. Acta 523 (2011) 84-89.
[88] Y. Han, H. Chen, N. Li, New incremental isoconversional method for kinetic analysis of solid thermal decomposition, J. Therm. Anal. Calorim. 104 (2011) 679-683.
[89] T. Dubaj, Z. Cibulkova, P. Simon, An incremental isoconversional method for kinetic analysis based on the orthogonal distance regression, J. Comput. Chem. 36 (2015) 392-398.
[90] K. Chen, S. Vyazovkin, Temperature dependence of sol-gel conversion kinetics in gelatinwater system, Macromol. Biosci. 9 (2009) 383-392.
[91] R. Farasat, B. Yancey, S. Vyazovkin, High Temperature Solid-solid Transition in Ammonium Chloride Confined to Nanopores, J. Phys. Chem. C 117 (2013) 13713-13721.
[92] V. L. Stanford, C. M. McCulley, S. Vyazovkin, Isoconversional kinetics of nonisothermal crystallization of salts from solutions, J. Phys. Chem. B 120 (2016) 5703-5709.
[93] T. Liavitskaya, S. Vyazovkin, Discovering the kinetics of thermal decomposition during continuous cooling, Phys. Chem. Chem. Phys. 18 (2016) 32021-32030.
[94] T. Liavitskaya, S. Vyazovkin, Kinetics of thermal polymerization can be studied during continuous cooling, Macromol. Rapid Commun. 39 (2018) 1700624.
[95] H. L. Friedman, Kinetics of thermal degradation of char-forming plastics from thermogravimetry. Application to a phenolic plastic, J. Polym Sci Part C 6 (1964) 183-195.
[96] P. Budrugeac, A simple and precise differential incremental isoconversional method to kinetic analysis of heterogeneous processes under arbitrary temperature programs, Thermochim. Acta, 661 (2018) 116-123.
[97] S.V. Vyazovkin, A.I. Lesnikovich, Practical application of isoconversional methods, Thermochim. Acta, 203 (1992) 177-185
[98] S. Vyazovkin, A unified approach to kinetic processing of nonisothermal data. Int. J. Chem. Kinet., 28 (1996) 95-101.
[99] D. Turnbull, J. C. Fisher, Rate of nucleation in condensed systems, J. Chem. Phys. 17 (1949) 71-73.
[100] T. Liavitskaya, L. Birx, S. Vyazovkin, Melting Kinetics of Superheated Crystals of Glucose and Fructose, Phys. Chem. Chem. Phys., 19 (2017) 26056-26064.
[101] K. Chen, A. N. Baker, S. Vyazovkin, Concentration effect on temperature dependence of gelation rate in aqueous solutions of methylcellulose. Macromol. Chem. Phys., 210 (2009) 211-216.
[102] S. Vyazovkin, N. Sbirrazzuoli, Isoconversional Kinetic Analysis of Thermally Stimulated Processes in Polymers, Macromol. Rapid Commun. 27 (2006) 1515-1532.
[103] J. D. Hoffman, J. I. Lauritzen, Jr. Crystallization of bulk polymers with chain folding: theory of growth of lamellar spherulites. J. Res. Natl. Bur. Stand. 65A (1961) 297-336.
[104] J. D. Hoffman, G. T. Davis, J. I. Lauritzen, Jr In: *Treatise on solid state chemistry, Vol. 3*; Ed.: N. B. Hannay, Plenum, NY, 1976, p. 497.
[105] S. Vyazovkin, N. Sbirrazzuoli, Isoconversional approach to evaluating the HoffmanLauritzen parameters (U^* and K_g) from the overall rates of nonisothermal melt crystallization, Macromol. Rapid Commun. 25(6) (2004) 733-738.
[106] S. Vyazovkin, I. Dranca, Isoconversional Analysis of Combined Melt and Glass Crystallization Data, Macromol. Chem. Phys. 207 (2006) 20-25.
[107] T. W. Chan, A. I. Isaev, Quiescent polymer crystallization: Modeling and measurements. Polym Eng Sci 34 ((1994) 461-471.
[108] A. Codou, N. Guigo, J. van Berkel, E. de Jong, N. Sbirrazzuoli, Nonisothermal Crystallization Kinetics of biobased Poly(ethylene 2,5-furandicarboxylate) synthesized via direct esterification process, Macromol. Chem. Phys. 215 (2014) 2065-2074.
[109] N. Bosq, N. Guigo, D. Aht-Ong, N. Sbirrazzuoli, Crystallization of Poly(butylene succinate) on Rapid Cooling and Heating: Toward Enhanced Nucleation by Graphene Nanosheets, J. Phys. Chem. C 121 (2017) 11915-11925.

[110] N. Bosq, N. Guigo, E. Zhuravlev, N. Sbirrazzuoli, Non-isothermal crystallization of polytetrafluoroethylene in wide range of cooling rates, J. Phys. Chem. B 117 (2013) 3407-3415.
[111] N. Bosq, N. Guigo, J. Persello, N. Sbirrazzuoli, Melt and glass crystallization of PDMS and PDMS silica nanocomposites, Phys. Chem. Chem. Phys. 16 (17) (2014) 7830 - 7840.
[112] N. Guigo, J. van Berkel, E. de Jong, N. Sbirrazzuoli, Modelling the non-isothermal crystallization of polymers:Application to poly(ethylene 2,5-furandicarboxylate), Thermochim. Acta 650 (2017) 66–75.
[113] M. R. Kamal, Thermoset characterization for moldability analysis, Polym. Eng. Sci. 14 (1974) 231-239.
[114] C. Alzina, N. Sbirrazzuoli, A. Mija, Hybrid nanocomposites: Advanced nonlinear method for calculating key kinetic parameters of complex cure kinetics, J. Phys. Chem. B 114 (2010) 12480-12487.
[115] A. Galukhin, T. Liavitskaya, S. Vyazovkin, Kinetic and Mechanistic Insights into Thermally Initiated Polymerization of Cyanate Esters with Different Bridging Groups, Macromol. Chem. Phys. 220 (2019) 1900141.
[116] N. Sbirrazzuoli, S. Vyazovkin, A. Mititelu, C. Sladic, L. Vincent, A Study of EpoxyAmine Cure Kinetics by Combining Isoconversional Analysis with Temperature Modulated DSC and Dynamic Rheometry, Macromol. Chem. Phys., 204 (2003) 1815-1821.
[117] G. van Assche, S. Swier, B. van Mele, Modeling and experimental verification of the kinetics of reacting polymer systems. Thermochim Acta 388 (2002) 327-341.
[118] S. Montserrat, X. Pla. Use of temperature-modulated DSC in kinetic analysis of a catalyzed epoxy-anhydride system, Polym. Int. 53 (2004) 326-331.
[119] I. Fraga, S. Montserrat and J. M. Hutchinson, Vitrification during the isothermal cure of thermosets. Part I. An investigation using TOPEM, a new temperature modulated technique, Journal of Thermal Analysis and Calorimetry 91 (2008) 687–695.
[120] E. Rabinowitch, Collision, co-ordination, diffusion and reaction velocity in condensed systems. Trans. Faraday Soc. 33 (1937) 1225-1233.
[121] A.M. Stolin, A.G. Merzhanov, A.Ya. Malkin, Non-isothermal phenomena in polymer engineering and science: a review -2. Non-isothermal phenomena in polymer deformation. Polym. Eng. Sci. 19 (1979) 1074-1080.
[122] N. Sbirrazzuoli, Advanced Isoconversional Kinetic Analysis for the Elucidation of Complex Reaction Mechanisms: A New Method for the Identification of Rate-Limiting Steps. Molecules 24 (2019) 1683.
[123] J. E. K. Schawe, A description of chemical and diffusion control in isothermal kinetics of cure kinetics. Thermochim Acta 388 (2002) 299-312.
[124] A.O. Konuray, X. Fernández-Francos X. Ramis, Analysis of the reaction mechanism of the thiol–epoxy addition initiated by nucleophilic tertiary amines. Polym. Chem. 8 (2017) 5934-5947.
[125] A.K. Galwey, M.E. Brown, Thermal Decomposition of Ionic Solids, Elsevier, Amsterdam, 1999.
[126] A.K. Galwey, Structure and order in thermal dehydrations of crystalline solids, Thermochim. Acta 355 (2000) 181-238.
[127] N. Koga, H. Tanaka, A physico-geometric approach to the kinetics of solid-state reactions as exemplified by the thermal dehydration and decomposition of inorganic solids, Thermochim. Acta 388 (2002) 41-61.
[128] N. Koga, Physico-geometric approach to the kinetics of overlapping solid-state reactions, in: S. Vyazovkin, N. Koga, C. Schick (Eds.) Handbook of Thermal Analysis and Calorimetry: Recent Advances, Techniques and Application, Elsevier, Amsterdam, 2018, pp. 213-251.
[129] M. Yoshikawa, Y. Goshi, S. Yamada, N. Koga, Multistep kinetic behavior in the thermal degradation of poly(L-lactic acid): A physico-geometrical kinetic interpretation, J. Phys. Chem. B 118 (2014) 11397-11405.
[130] N. Kameno, S. Yamada, T. Amimoto, K. Amimoto, H. Ikeda, N. Koga, Thermal degradation of poly(lactic acid) oligomer: Reaction mechanism and multistep kinetic behavior, Polym. Degrad. Stab. 134 (2016) 284-295.
[131] N. Koga, Y. Goshi, S. Yamada, L.A. Pérez-Maqueda, Kinetic approach to partially overlapped thermal decomposition processes, J. Therm. Anal. Calorim. 111 (2013) 1463-1474.

[132] J. Šesták, G. Berggren, Study of the kinetics of the mechanism of solid-state reactions at increasing temperatures, Thermochim. Acta 3 (1971) 1-12.
[133] L.A. Pérez-Maqueda, J.M. Criado, J. Málek, Combined kinetic analysis for crystallization kinetics of non-crystalline solids, J. Non. Cryst. Solids 320 (2003) 84-91.
[134] L.A. Pérez-Maqueda, J.M. Criado, P.E. Sánchez-Jiménez, Combined kinetic analysis of solid-state reactions: A powerful tool for the simultaneous determination of kinetic parameters and the kinetic model without previous assumptions on the reaction mechanism, J. Phys. Chem. A 110 (2006) 12456-12462.
[135] P.E. Sánchez-Jiménez, L.A. Pérez-Maqueda, A. Perejón, J.M. Criado, Combined kinetic analysis of thermal degradation of polymeric materials under any thermal pathway, Polym. Degrad. Stab. 94 (2009) 2079-2085.
[136] N. Koga, H. Tanaka, A kinetic compensation effect established for the thermal decomposition of a solid, J. Therm. Anal. 37 (1991) 347-363.
[137] N. Koga, J. Šesták, Kinetic compensation effect as a mathematical consequence of the exponential rate constant, Thermochim. Acta 182 (1991) 201-208.
[138] N. Koga, J. Šesták, Further aspects of the kinetic compensation effect, J. Therm. Anal. 37 (1991) 1103-1108.
[139] N. Koga, A review of the mutual dependence of Arrhenius parameters evaluated by the thermoanalytical study of solid-state reactions: The kinetic compensation effect, Thermochim. Acta 244 (1994) 1-20.
[140] A.K. Galwey, M. Mortimer, Compensation effects and compensation defects in kinetic and mechanistic interpretations of heterogeneous chemical reactions, Int. J. Chem. Kinet. 38 (2006) 464-473.
[141] D. Xu, M. Chai, Z. Dong, M.M. Rahman, X. Yu, J. Cai, Kinetic compensation effect in logistic distributed activation energy model for lignocellulosic biomass pyrolysis, Biorecour. Technol. 265 (2018) 139-145.
[142] N. Koga, Y. Yamane, Effect of mechanical grinding on the reaction pathway and kinetics of the thermal decomposition of hydromagnesite, J. Therm. Anal. Calorim. 93 (2008) 963-971.
[143] J. Cai, R. Liu, Weibull mixture model for modeling nonisothermal kinetics of thermally stimulated solid-state reactions: application to simulated and real kinetic conversion data, J. Phys. Chem. B 111 (2007) 10681-10686.
[144] J. Cai, S. Alimujiang, Kinetic analysis of wheat straw oxidative pyrolysis using thermogravimetric analysis: Statistical description and isoconversional kinetic analysis, Ind. Eng. Chemi. Res. 48 (2009) 619-624.
[145] A. Perejon, P.E. Sanchez-Jimenez, J.M. Criado, L.A. Perez-Maqueda, Kinetic analysis of complex solid-state reactions. A new deconvolution procedure, J. Phys. Chem. B 115 (2011) 1780-1791.
[146] R. Svoboda, J. Málek, Applicability of Fraser–Suzuki function in kinetic analysis of complex crystallization processes, J. Therm. Anal. Calorim. 111 (2013) 1045-1056.
[147] A. Ambekar, J.J. Yoh, Kinetics deconvolution study of multi-component pyrotechnics, Thermochim. Acta 667 (2018) 27-34.
[148] F.J. Gotor, J.M. Criado, J. Málek, N. Koga, Kinetic analysis of solid-state reactions: The universality of master plots for analyzing isothermal and nonisothermal experiments, J. Phys. Chem. A 104 (2000) 10777-10782.
[149] J.M. Criado, L.A. Pérez-Maqueda, F.J. Gotor, J. Málek, N. Koga, A unified theory for the kinetic analysis of solid state reactions under any thermal pathway, J. Therm. Anal. Calorim. 72 (2003) 901-906.
[150] T. Wada, N. Koga, Kinetics and mechanism of the thermal decomposition of sodium percarbonate: Role of the surface product layer, J. Phys. Chem. A 117 (2013) 1880-1889.
[151] T. Wada, M. Nakano, N. Koga, Multistep kinetic behavior of the thermal decomposition of granular sodium percarbonate: Hindrance effect of the outer surface layer, J. Phys. Chem. A 119 (2015) 9749-9760.
[152] S. Iwasaki, S. Kodani, N. Koga, Physico-geometrical kinetic modeling of the thermal decomposition of magnesium hydroxide, J. Phys. Chem. C 124 (2020) 2458-2471.

[153] N. Koga, S. Kodani, Thermally induced carbonation of Ca(OH)2 in a CO2 atmosphere: Kinetic simulation of overlapping mass-loss and mass-gain processes in a solid-gas system, Phys. Chem. Chem. Phys. 20 (2018) 26173-26189.
[154] Y. Noda, N. Koga, Phenomenological kinetics of the carbonation reaction of lithium hydroxide monohydrate: Role of surface product layer and possible existence of a liquid phase, J. Phys. Chem. C 118 (2014) 5424-5436.
[155] S. Kitabayashi, N. Koga, Thermal decomposition of tin(II) oxyhydroxide and subsequent oxidation in air: Kinetic deconvolution of overlapping heterogeneous processes, J. Phys. Chem. C 119 (2015) 16188-16199.
[156] N.V. Muravyev, N. Koga, D.B. Meerov, A.N. Pivkina, Kinetic analysis of overlapping multistep thermal decomposition comprising exothermic and endothermic processes: thermolysis of ammonium dinitramide, Phys. Chem. Chem. Phys. 19 (2017) 3254-3264.
[157] N.V. Muravyev, A.N. Pivkina, N. Koga, Critical appraisal of kinetic calculation methods applied to overlapping multistep reactions, Molecules 24 (2019) 2298.
[158] K.L. Mampel, Time conversion formulas for heterogeneous reactions at the phase boundaries of solid bodies. I: The development of the mathematical method and the derivation of area conversion formulas, Z. Phys. Chem. Abt. A 187 (1940) 43-57.
[159] L. Favergeon, M. Pijolat, M. Soustelle, Surface nucleation and anisotropic growth models for solid-state reactions, Thermochim. Acta 654 (2017) 18-27.
[160] M. Pijolat, L. Favergeon, Kinetics and mechanisms of solid-gas reactions, in: S. Vyazovkin, N. Koga, C. Schick (Eds.) Handbook of Thermal Analysis and Calorimetry: Recent Advances, Techniques and Applications, Elsevier, Amsterdam, 2018, pp. 173-212.
[161] H. Ogasawara, N. Koga, Kinetic modeling for thermal dehydration of ferrous oxalate dihydrate polymorphs: A combined model for induction period-surface reaction-phase boundary reaction, J. Phys. Chem. A 118 (2014) 2401-2412.
[162] S. Kitabayashi, N. Koga, Physico geometrical mechanism and overall kinetics of thermally induced oxidative decomposition of tin(II) oxalate in air: formation process of microstructural tin(IV) oxide, J. Phys. Chem. C 118 (2014) 17847-17861.
[163] M. Fukuda, N. Koga, Kinetics and mechanisms of the thermal decomposition of copper(II) hydroxide: A consecutive process comprising induction period, surface reaction, and phase boundary-controlled reaction, J. Phys. Chem. C 122 (2018) 12869-12879.
[164] N. Koga, L. Favergeon, S. Kodani, Impact of atmospheric water vapor on the thermal decomposition of calcium hydroxide: A universal kinetic approach to a physico-geometrical consecutive reaction in solid-gas systems under different partial pressures of product gas, Phys. Chem. Chem. Phys. 21 (2019) 11615-11632.
[165] M. Fukuda, L. Favergeon, N. Koga, Universal kinetic description for thermal decomposition of copper(II) hydroxide over different water vapor pressures, J. Phys. Chem. C 123 (2019) 20903-20915.
[166] L.A. Pérez-Maqueda, J.M. Blanes, J. Pascual, J.L. Perez-Rodriguez, The influence of sonication on the thermal behavior of muscovite and biotite, J. Eur. Ceram. Soc. 24 (2004) 2793-2801.
[167] E. Gil-González, A. Perejón, P.E. Sánchez-Jiménez, S. Medina-Carrasco, J. Kupčík, J. Šubrt, J.M. Criado, L.A. Pérez-Maqueda, Crystallization kinetics of nanocrystalline materials by combined X-ray diffraction and differential scanning calorimetry experiments, Cryst. Growth Des. 18 (2018) 3107-3116.

GLOSSARY

Autocatalytic reactions as well as autoaccelerating. Reactions whose rate under isothermal conditions passes through a maximum. Consequentially, the integral curves α vs t have sigmoidal shape so that the respective reactions and kinetics are also referred to as sigmoidal. They are commonly described by the Avrami or truncated Šesták-Berggren (extended Prout-Tompkins) model.

Coefficient of determination (r^2) is square of the Pearson's correlation coefficient, r.

Convolution is a mathematical operation of combining two functions into one via the convolution integral. Convolution is distinctly different from the addition of two functions. For example, convolution of two Gaussian peak functions does not yield a double peak, but another Gaussian peak function.

Decelerating reactions. Reactions whose rate under isothermal conditions continuously decreases. They are commonly described by the reaction-order or diffusion models.

Deconvolution is a mathematical operation of separating of a convolved function into individual functions. It is commonly accomplished by the Fourier transform. Representative examples are: in signal analysis, separation of noisy signals into noise and signal; in atomic spectroscopy, separation of the true spectral peak from the effects of the Doppler and pressure broadening; in calorimetry, separation of the sample heat flow from the instrument response function. Although not strictly correct, the term is now commonly used for curve resolution or curve separation for overlapped multiple peaks observed in spectroscopy or in thermal analysis kinetics.

Effective activation energy as well as effective rate constant or other effective kinetic parameters. "Effective" is used to emphasize that this is not merely theoretical but the actual, i.e., acting in reality value. In this meaning, "Effective" is synonymous with "Global", "Overall", "Apparent", "Experimental".

Extent of conversion, degree of conversion, conversion, extent of reaction. Commonly denoted by α and defined as the ratio of the partial to total change of a physical property. For example, the ratio of the partial mass loss at given temperature to the total mass loss at the final temperature.

Kinetic curve, kinetic data. Terms commonly used to describe dependencies of α or $d\alpha/dt$ on time or temperature.

Kinetic parameters. In addition to the activation energy and preexponential factor, this terms usually includes parameters of the reaction models, e.g., the exponents in the Avrami, reaction order, and Šesták-Berggren models.

Multi-step kinetic model (e.g., double-step kinetic model), model containing more than one kinetic step. In such model, each step has its individual reaction model (i.e., $f(\alpha)$) and the steps have specific connections to each other, e.g., parallel or consecutive.

Multi-step kinetics, kinetics whose overall rate is determined by the rates of more than one step.

Reaction model or kinetic model, a function that represents the conversion dependence of the rate, i.e., $f(\alpha)$ (or its integral analog, $g(\alpha)$)

Reaction order model, *n*th-order reaction. Reactions or models that are represented by the kinetic model $f(\alpha)=(1-\alpha)_n$.

Reaction profile. Same as **kinetic curve**.

Residual sum of squares (RSS). RSS is a quantity used in the method of least squares to represent the minimum of squared deviations between an experimental dependence and its theoretical model. RSS is a statistical quantity similar to the variance and, thus, can be analyzed by the F- and χ_2- tests.

Single-step kinetics, kinetics whose overall rate is determined by the rate of one step.